C. R. Physique 14 (2013) 667–684

Contents lists available at ScienceDirect

Comptes Rendus Physique

www.sciencedirect.com

Disordered systems / Systèmes désordonnés

Nanoscale studies of ferroelectric domain walls as pinned elastic interfaces

Études nanoscopiques de parois de domaines ferroélectriques comme interfaces élastiques piégées

Patrycja Paruch *, Jill Guyonnet

MaNEP–DPMC, Université de Genève, 24, quai Ernest-Ansermet, 1211 Geneva, Switzerland

ARTICLE INFO

Article history:
Available online 7 September 2013

Keywords:
Domain walls
Piezoresponse force microscopy
Creep
Roughness
Disorder
Out-of-equilibrium

Mots-clés :
Parois de domaines
Microscopie à force atomique en mode piézoréponse
Reptation
Rugosité
Désordre
Hors équilibre

ABSTRACT

The competition between elasticity and pinning of an interface in a fluctuating potential energy landscape gives rise to characteristic self-affine roughening and a complex dynamic response to applied forces. This statistical physics approach provides a general framework in which the behaviour of systems as diverse as propagating fractures, wetting lines, burning fronts or surface growth can be described. Domain walls separating regions with different polarisation orientation in ferroelectric materials are another example of pinned elastic interfaces, and can serve as a particularly useful model system. Reciprocally, a better understanding of this fundamental physics allows key parameters controlling domain switching, growth, and stability to be determined, and used to improve the performance of ferroelectric materials in applications such as memories, sensors, and actuators. In this review, we focus on piezoresponse force microscopy measurements of individual ferroelectric domain walls, allowing their static configuration and dynamic response to be accessed with nanoscale resolution over multiple orders of length scale and velocity. Combined with precise control over the applied electric field, temperature, and strain, and the ability to influence the type and density of defects present in the sample, this experimental system has allowed not only a direct demonstration of creep motion and roughening, but provides an opportunity to test less-well-understood aspects of out-of-equilibrium behaviour, and the effects of greater complexity in the structure of both the interface and the disorder landscape pinning it.

RÉSUMÉ

La compétition entre l'élasticité d'une interface et le piégeage par un potentiel désordonné confère à cette dernière une configuration rugueuse auto-affine caractéristique ainsi qu'une réponse dynamique complexe aux forces externes. Cette approche de physique statistique fournit une description théorique générale du comportement de systèmes aussi divers que la propagation de fractures, les lignes de mouillage, les fronts de combustion et les phénomènes de croissance de surface. Dans les matériaux ferroélectriques, les parois de domaines, qui séparent les régions où la polarisation est orientée différemment, forment un autre exemple d'interfaces élastiques piégées, et constituent à ce titre un système modèle particulièrement utile. Réciproquement, une meilleure compréhension de ces propriétés physiques fondamentales permet de déterminer les paramètres-clés contrôlant

* Corresponding author.
E-mail address: Patrycja.Paruch@unige.ch (P. Paruch).

1631-0705/$ – see front matter
http://dx.doi.org/10.1016/j.crhy.2013.08.004

la nucléation, la croissance et la stabilité des domaines et, de ce fait, l'amélioration des performances des matériaux ferroélectriques pour des applications telles que mémoires, senseurs et actionneurs. Dans cette revue, nous nous focalisons sur des mesures de parois de domaines ferroélectriques individuelles par microscopie à force atomique en mode piézoréponse, qui permettent de déterminer leur configuration statique et leur réponse dynamique avec une résolution nanométrique sur plusieurs ordres de grandeur de longueur et de vitesse. Combiné au contrôle précis du champ électrique appliqué, de la température, de la contrainte, et de la nature et densité des défauts présents dans l'échantillon, ce système expérimental permet non seulement une démonstration directe des phénomènes de reptation et de rugosité, mais également d'appréhender certains aspects moins connus de phénomènes hors équilibre ainsi que les effets dúne structure plus complexe, tant au niveau de l'interface elle-même que du potentiel désordonné de piégeage.

1. Introduction

Ferroelectric materials are characterised by symmetry-equivalent ground states with different orientation of the non-volatile macroscopic electric dipole moment, or polarisation, which may be switched by the application of an external electric field. Depending on the strain and electrostatic boundary conditions, as well as its switching history, a sample may present a uniformly polarised configuration, or coexisting regions with different polarisation orientation, known as domains, separated by domain walls [1–3]. As thin as 1–2 unit cells (<1 nm) [4,5], the domain walls, shown in Fig. 1, can be thought of as extended topological defects, with different electronic and structural symmetry from their parent materials as a result of the rotation or local absence of polarisation. The application of an external electric field along the polarisation axis asymmetrises the ferroelectric double-well potential, and promotes the growth of domains with the preferred orientation, thus driving domain wall motion.

Understanding the static and dynamic behaviour of domain walls, and specifically their interaction with commensurate (crystal lattice) or random (defects/disorder) pinning sites is key to predicting and controlling domain switching, growth and stability, all questions of high technological as well as fundamental interest. In particular, the switchable remanent polarisation, together with associated pyroelectric and piezoelectric properties, has led to the integration of ferroelectrics in devices ranging from memories [6,7] to micro- and nano-electromechanical sensors and actuators [8–10], and numerous electro-optic applications [11]. In addition, recent discoveries of unusual functional properties localised specifically at the domain walls [12–14] make them extremely promising as potential active device components in a future domain-wall-based nanoelectronics.

From a theoretical point of view, the effects of complex, heterogeneous disorder inherent to real samples at multiple orders of length scales are difficult to incorporate explicitly. Analytical solutions of Ginzburg–Landau mean-field-type calculations provide invaluable information about the thermodynamics and kinetics of defect-free domain switching [15–18], and models of domain walls [3] and their interactions with single defects [19], or with particularly regular, periodically ordered pinning potentials [20], but do not readily describe the inherent randomness. First-principles atomistic simulations, meanwhile, give extremely accurate estimates of domain wall energies and interactions with individual defects [4,21–23], but do not easily scale up beyond super cells of hundreds of atoms. Rather, to tackle the effects of random fluctuations at multiple length scales, a statistical description is necessary. Such a statistical, highly reductionist approach to domain walls within the general framework of disordered elastic systems has proven very powerful, allowing metastability and the glassy physics associated with an energy landscape characterised by multiple local minima to be addressed [24–26]. Conversely, as a result of the high resolution of scanned probe microscopy, combined with access to a broad range of control parameters such as the applied electric field, temperature, environmental (electrochemical) and strain boundary conditions, ferroelectric domain walls present a useful model system for testing theoretical predictions about pinned elastic interfaces.

Within this framework, the behaviour of such interfaces is governed by the competition between elasticity, which tends to flatten the interface, and pinning, due to fluctuations in the potential energy landscape, leading to roughening and a complex response to an applied force. The scaling of the roughness in the static equilibrium configuration, as well as of the quasi-static thermally activated dynamics for low driving forces, and of the transition to depinning at higher forces, are universal phenomena characterised by exponents whose values are linked to the dimensionality of the system and the universality class of the disorder. Although the equilibrium properties of such systems are relatively well established, much less is known about their out-of-equilibrium behaviour, including ageing and memory effects. In addition, the interaction of an interface with a more complex, highly heterogeneous disorder landscape, as well as the consequences of its potentially intricate internal structure remain poorly understood. Ferroelectric domain walls in epitaxial perovskite (multi)ferroic thin films, with potentially complex internal structure and coupling between different order parameters, and where a variety of defects can be introduced during or after growth can therefore allow these intriguing phenomena to be investigated, and form the subject of this review.

We begin with an overview of the physics of elastic interfaces in disordered media in Section 2, then discuss in Section 3 how this theoretical framework was specifically applied to ferroelectric domain walls, with initial indications of domain

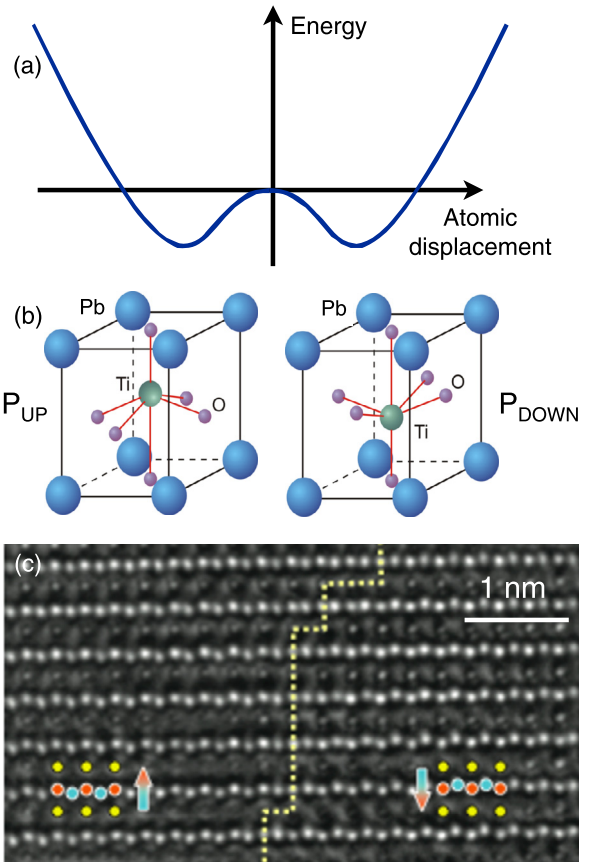

Fig. 1. Domain walls in ferroelectric materials. (a) The ferroelectric free energy as a function of atomic displacements from a reference, high-symmetry paraelectric phase, characterised by symmetry-equivalent, oppositely polarised ground states separated by an energy barrier. (b) Schematic representation of the antagonistic displacements of the positively charged Pb and Ti atoms, and the negatively charged O atoms in a unit cell of the canonical tetragonal ferroelectric $PbTiO_3$, giving rise to up- and down-oriented polarisation states. (c) Transmission electron micrograph of a 180° domain wall separating a P_{UP} and P_{DOWN} polarised region in a thin film of $Pb(Zr,Ti)O_3$, adapted from [5]. The atomic displacements differ from their bulk value, indicated left and right of the dotted yellow line marking the central wall plane, across only approximately 2 unit cells. Colour available on the web.

wall pinning in macroscopic functional measurements, followed by detailed nanoscopic studies of the static and dynamic behaviour of individual domain walls, which are the main focus of the present review. In Section 4 we relate more recent research, addressing the effects of heterogeneous disorder, the consequences of complex internal domain wall structure, and the still-open question of out-of-equilibrium behaviour, with ageing and memory effects.

2. The static and dynamic behaviour of pinned elastic interfaces

In the absence of other influences, an interface with short-range elasticity will optimise its elastic energy $H_{el} \sim \int (\nabla_z u(\mathbf{z}))^2 \, \mathrm{d}^d z$ by limiting distortions $\nabla_z u(\mathbf{z})$ from a flat configuration. However, variations in the potential energy landscape in the presence of finite temperature (T) thermal fluctuations, or due to defects (disorder), or an underlying crystal lattice periodicity can act as pinning sites with energy H_{pin} and promote wandering. This competition between elasticity and pinning $H = H_{el} + H_{pin}$ results in a glass-like physics, evident in both the characteristic roughening and complex dynamic behaviour of the system.[1]

Across a ferroelectric domain wall, the increased energy density σ_{DW} associated with the extremely localised rotation and/or change in magnitude of the polarisation can be seen as a short-range elasticity, and the domain walls can therefore be considered as elastic interfaces, with an optimal flat, minimal surface (two-dimensional domain walls in three-dimensional bulk samples) or line-length (one-dimensional domain walls in two-dimensional thin films) configuration. In real ferroelectric systems, the pinning potential for domain walls can be extremely complex and heterogeneous, with point as well as extended structural and electric defects, both random and correlated, coexisting in a given sample with the underlying commensurate pinning potential of the crystal lattice. Also, individual defects can act as strong pinning centres,

[1] For a more detailed treatment, we invite the interested reader to consult the excellent text by Barabasi and Stanley [27], and reviews by Blatter et al. [28], Giamarchi et al. [25], and Agoritsas et al. [29].

potentially resulting in a multivalued domain wall configuration with islands and overhangs, or multiple weak point defects can act collectively, giving rise to a univalued domain wall configuration which depends rather on fluctuations in defect density than on the specific positions of individual defects.

2.1. Static roughness of pinned elastic interfaces

In the case of weak pinning by uncorrelated disorder, more tractable from a statistical theory point of view, the equilibrium roughening at a given length scale r is formally described by the relative displacements $\Delta u(r) = u(z) - u(z+r)$ from the flat elastically optimal configuration, where the transverse displacements $u(z)$ are measured along the longitudinal coordinate z, as shown in Fig. 2a. The relative displacements grow for increasing scales r, with characteristic universal scaling accessed in real space via the effective width:

$$W(r) = \overline{\left\langle \left[u(z) - \langle u \rangle_r\right]^2 \right\rangle_r}^{1/2} \sim r^{\zeta} \tag{1}$$

or the roughness:

$$B(r) = \overline{\left\langle \left[\Delta u(r)\right]^2 \right\rangle_r}^{1/2} \sim r^{2\zeta} \tag{2}$$

of the interface, or in reciprocal space by its structure factor:

$$S(q) = \left\langle \left|u(q)\right|^2 \right\rangle \sim q^{-(1+2\zeta)} \tag{3}$$

where $u(q)$ is the Fourier transform of the displacement field $u(z)$, and $\langle \ldots \rangle$, $\overline{\ldots}$ denote an average over z, and an average over disorder realisations, respectively. The specific value of the roughness exponent ζ depends on the system dimensionality d, the nature of the disorder, and the range of the elastic interactions. For disorder in the random bond universality class (Fig. 2b), which in the case of ferroelectric domain walls corresponds to defects locally varying the depth of the double-well ferroelectric potential, without changing its symmetry, $\zeta = 2/3$ for one-dimensional interfaces and $\zeta \approxeq 0.2084(4-d)$ for $(d>1)$-dimensional interfaces. For random field disorder (Fig. 2c), corresponding to defects that locally asymmetrise the ferroelectric double-well potential, $\zeta = 1$ for all dimensionalities $d < 4$. In the case of purely thermal fluctuations $\zeta = 1/2$ for one-dimensional interfaces.

For real interfaces such as ferroelectric domain walls, additional effects including finite interface thickness ξ and long range dipolar interactions need to be taken into account. Thus, at very short length scales $r < r_C$, below which $\Delta u(r) < \xi$, the scaling of the displacement field is actually dominated by elasticity, and the interface is in the Larkin regime with $B(r) \sim r^{4-d}$. The critical length scale r_C is known as the Larkin length. At higher length scales $r > r_C$, $\Delta u(z) > \xi$, disorder effects dominate, and the interface properly enters the random manifold regime, with $B(r) \sim r^{2\zeta}$, as can be seen in Fig. 2d. With finite temperatures, the effective thickness of the interface increases $\xi_{\mathrm{eff},T>0} > \xi_{T=0}$ as a result of the induced thermal jitter [30], allowing continual exploration of the pinning potential landscape at energy scales $\sim k_B T$. Meanwhile, due to dipolar interactions, the stiffness of the interface, and thus its elasticity under deformations perpendicular to the polar orientation is higher than that for deformations along the polar orientation. For 180° ferroelectric domain walls, for example, such effects need to be taken into account at length scales for which the domain wall may be considered as a two-dimensional interface in a three-dimensional sample. In this case, the elastic energy (expressed in reciprocal space), contains not only the short-range term:

$$H_{\mathrm{el}} = \frac{1}{2}\sum_q C_{\mathrm{el}}(q) u^*(q) u(q) \tag{4}$$

with $C_{\mathrm{el}}(q) = \sigma_{\mathrm{DW}} q^2$, but also the dipolar interaction with:

$$C_{\mathrm{dp}} = \frac{2P_s^2}{\epsilon_0 \epsilon}\frac{q_y^2}{q} + \frac{P_s^2 \xi}{\epsilon_0 \epsilon}\left(\frac{-3}{4}q_x^2 + \frac{1}{8}q^2\right) \tag{5}$$

where P_s is the ferroelectric polarisation along direction y, and ϵ and ϵ_0 are the relative and vacuum dielectric constants. Because q_y now scales as $q_y \sim q_x^{3/2}$, an effective dimensionality $d_{\mathrm{eff}} = d + 1/2$ needs to be used to determine the expected values of ζ for random bond and random field disorder [31,32].

A higher effective dimensionality likewise needs to be considered for interacting ferroelectric domain walls in periodic domain arrays. Such structures occur intrinsically when insulating or weakly metallic boundary conditions on the free faces of a ferroelectric thin film, combined with few available free charges, lead to the presence of uncompensated dipoles at the surface. The associated electrostatic energy cost can be reduced by the creation of domains with opposite polarity, allowing local field closure across the domain walls. Optimising the volume energy density of the domain U_D vs. the surface density of the domain wall σ_{DW} gives rise to a characteristic Landau–Lifshitz–Kittel [33,34] scaling of domain periodicity $w_D = \sqrt{\sigma_{DW} h_S / U_D}$ with the sample thickness h_S. In this case, as for the Bragg glass of magnetic vortices in a disordered lattice [35], the dimensionality which determines the values of the roughness exponent becomes that of the entire system $d_{\mathrm{eff}} = d + m$ rather than that of an individual interface (d) with an $m = 1$ dimensional displacement field. Moreover, as

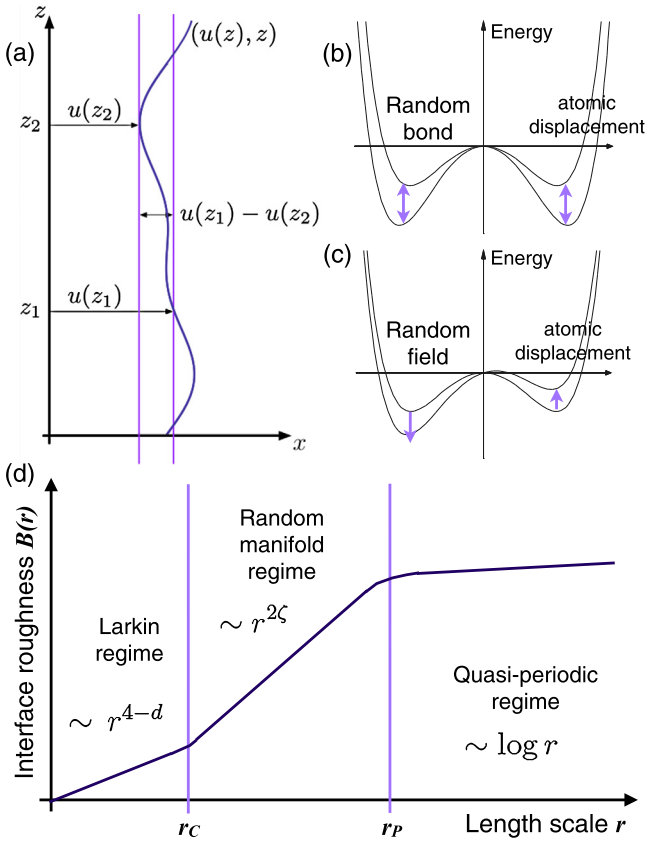

Fig. 2. Equilibrium roughening of pinned elastic interfaces. (a) Relative displacement $\Delta u(r)$ for $r = z_2 - z_1$ of a one-dimensional interface from its flat, elastically optimal configuration under the influence of weak collective pinning in a disorder potential, adapted from [29]. (b) Random bond disorder preserves the symmetry of the double-well potential, while locally changing its depth. (c) Random field disorder corresponds to local internal fields, which asymmetrise the ferroelectric double-well potential. (d) The roughness $B(r)$ of the interface grows with the length scale r, adapted from [29]. For short length scales dominated by elasticity, $B(r) \sim r^{4-d}$. At higher length scales, an individual interface weakly pinned by a random potential shows mono-affine scaling characterised by universal exponents, with $B(r) \sim r^{2\zeta}$. In a periodic system of interacting interfaces, roughening slows significantly at length scales corresponding to relative displacements of the order of the system periodicity, with $B(r) \sim \log r$.

the relative displacements $\Delta u(r)$ approach the characteristic periodicity of the system r_P, roughening slows significantly to $B(r > r_P) \sim \log r$, as shown schematically in Fig. 2d.

In the case of more general disorder, it may also be necessary to consider all the n-th order moments of the probability distribution function (PDF) of relative displacements $\Delta u(r)$, which reflect the characteristic scaling properties of the system [29]:

$$M_n(r) = \overline{\left\langle \left| \Delta u(r) \right|^n \right\rangle} \sim r^{n\zeta_n} \tag{6}$$

where ζ_n are the associated scaling exponents. For the mono-affine case of weak pinning by uncorrelated disorder, the interfacial roughening presents a Gaussian PDF of relative displacements [36–38], and the second moment $S_2(r) \equiv B(r)$ fully describes the scaling properties of the static configuration, with a single-valued roughness exponent $\zeta_n = \zeta \ \forall n$. This is not necessarily the case for more complex disorder models [39], which have shown multi-affine behaviour characterised by an infinite set of individual scaling exponents ζ_n and a hierarchy of local roughness exponents.

2.2. Complex dynamic response of pinned elastic interfaces

The competition between elasticity and pinning likewise governs the dynamic behaviour of the system, giving rise to a complex response to applied forces, as shown schematically in Fig. 3a. With no thermal activation at $T = 0$, the interface remains pinned until the applied force reaches a critical depinning threshold F_C, then responds with abruptly rising velocity v. This behaviour strongly resembles the evolution of the order parameter during a second order phase transition, and for which, by analogy, universal scaling $v \sim (F - F_C)^\theta$ may be expected. At high driving forces, when the interface energy is well above the microscopic details of the disorder landscape, standard linear flow is recovered with $v \sim F$, with the pinning contributing essentially a viscous drag. In real systems at finite temperature $T > 0$, the sharp depinning transition becomes

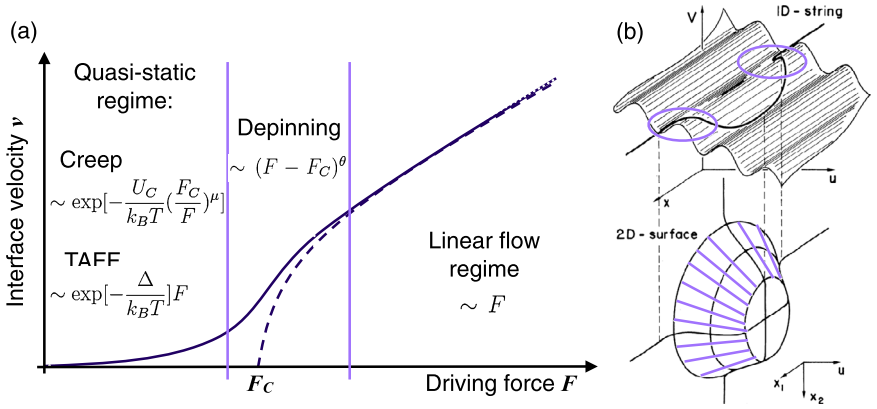

Fig. 3. The complex dynamic response of a pinned elastic interface. (a) Interface velocity v as a function of the driving force F, adapted from [29]. At zero temperature (dashed curve), the interface remains pinned until a critical force F_C is reached. Thermally activated ultra-slow motion is possible even for subcritical forces at finite temperature (solid curve). At high driving forces, standard linear response is recovered. (b) For an interface driven in a periodic pinning potential, the cost of an excursion into an adjacent potential minimum is bounded for one-dimensional interfaces, and grows as the surface of a two-dimensional interface, leading to creep-like dynamics in the latter case, adapted from [28].

thermally rounded [40]. Thermal activation also allows a quasi-static response to subcritical forces $F \ll F_C$, where the energy optimisation as a segment of the interface is displaced in the corresponding conjugate field must be balanced against the energy cost of increased interface surface, as well as depolarising and dipolar energies, as appropriate. If the pinning barriers are finite, with some typical energy Δ, thermally assisted flux flow is expected, with a linear but exponentially small response

$$v \sim \exp\left[-\frac{\Delta}{k_B T}\right]F \tag{7}$$

If, however, the energy barriers diverge as $F \to 0$, with

$$U_B(F) \sim \left(\frac{1}{F}\right)^{\frac{d-2+2\zeta}{2-\zeta}} \tag{8}$$

as in the case of randomly pinned glassy systems, the result is rather a highly non-linear creep motion:

$$v \sim \exp\left[-\frac{U_C}{k_B T}\left(\frac{F_C}{F}\right)^{\mu}\right] \tag{9}$$

where U_C is a characteristic energy scale. The creep exponent μ depends on the dimensionality of the system and the universality class of the disorder:

$$\mu = \frac{d-2+2\zeta}{2-\zeta} \tag{10}$$

In the case of a ferroelectric domain wall in a commensurate pinning potential, such as that of the underlying crystal lattice [4], the resulting energy landscape can be seen as a tilted washboard [28], as shown in Fig. 3b. For $d = 2$ domain walls, the energy gain grows with the volume of the nucleus, and the energy cost with its surface. This energy balance leads to the well known Miller–Weinreich [41] equation of domain wall motion in an electric field E, which shows non-linear glassy characteristics with $v \sim \exp[-\frac{U_{D,DW}}{k_B T E}]$, where $U_{D,DW}$ takes into account both the electrostatic and domain wall energies. This expression, developed from observations of domain wall motion in optical-etching studies of single crystals [42,43], has also been confirmed by numerical simulations of the formation of a critical nucleus at an existing domain wall in a defect-free material [44]. For $d = 1$ domain walls, the energy gain scales with the length of the nucleus, while the energy cost is finite, giving rise to thermally assisted flux flow $v \sim \exp[-\frac{\Delta}{k_B T}]E$, or $v \sim \exp[-\frac{\Delta}{k_B T}]E^n$ in the limiting case. However, when pinning in a random disorder potential is considered, both 1- and 2-dimensional domain walls should show creep motion $v \sim \exp[-\frac{U_C}{k_B T}(\frac{1}{E})^{\mu}]$ characteristic of glassy systems.

3. Ferroic domain walls as pinned elastic interfaces

During the initial intense period of research on ferroelectric perovskites from mid-20th century onwards, fundamental studies focused primarily on single crystals, for benchmark measurements of their switching properties and domain structure and stability. Industrial research, meanwhile, turned to ceramics – cheap and readily processed for integration in a wide

array of technological applications, ranging from piezoelectric electromechanical transducers and dielectric sensors to prototype radiation-hard memories [9,6]. Although the effects of defects were clearly recognised as crucial, they were difficult to include explicitly in the mean-field Ginzburg–Landau–Devonshire approach. Phenomenological theories of domain switching [45,46] implicitly included the influence of a random potential landscape by assuming stochastic nucleation events, while domain wall motion during subsequent domain growth was posited to be constant and uniform.

The domain walls themselves were considered as essentially straight, with competition between the energy cost of domain wall and the depolarising field leading to the formation of periodic domains showing the characteristic Landau–Lifshitz–Kittel scaling with the thickness of the material [33,34]. Optical studies in single crystals suggested that the predominant factor determining domain wall configuration was the crystal lattice potential: the domain walls indeed appeared straight or strongly faceted, and were often aligned along axes of crystalline symmetry [2,47]. Likewise, early studies of domain growth agreed very well with the Miller–Weinreich description of domain wall dynamics [41–43], implicitly based on the effect of a commensurate pinning potential.

3.1. Evidence of domain wall (de)pinning in macroscopic functional measurements

A seminal contribution was the work of Nattermann et al., specifically applying the formalism of disordered elastic systems to domain walls to consider the effects of commensurate vs. random pinning [32,48], random bond vs. random field disorder [49,50], and the effects of long range dipolar interactions [31], suggesting susceptibility measurements in ferroic systems as a way to access domain wall (de)pinning and creep dynamics at a macroscopic level.

This insight was particularly important for studies of functional properties in ferroelectric thin films and ceramics [51], where features analogous to the Rayleigh law for magnetic susceptibility could only be explained by (de)pinning of domain walls in a random potential. In standard ferroelectrics such as $Pb(Zr,Ti)O_3$, dielectric [52,53] and piezoelectric [54,55] measurements suggested structural defects and thus random bond pinning as the dominant mechanism. In relaxor ferroelectric such as $Sr_{0.61-x}Ce_xBa_{0.39}Nb_2O_6$ or KH_2PO_4, on the other hand, optical dielectric measurements were compatible with random field disorder [56–58]. In such materials, where fluctuations of the potential landscape can be directly related to the presence of randomly oriented polar nanoregions, random-field pinning would indeed be expected. Although some reports initially posited a slow dynamics varying linearly with the driving force to explain the non-Debye contributions to the dielectric response, where the effect of random pinning was included only as a broad distribution of domain wall mobilities [59], consensus supporting the actual non-linear creep dynamics gradually emerged [60,61]. In periodically poled $KTiOPO_4$, susceptibility measurements of domain wall creep with $\mu = 1$ were reported, and also linked to pinning by weak disorder, in this case due to cationic superionicity [62]. Direct pinning and bowing of a single domain wall under a uniform applied electric field was also observed optically at the 1–10 μm level [63].

3.2. Using PFM to study individual ferroelectric domain walls

Piezoresponse force microscopy (PFM) allows the nanoscale imaging of individual domain walls and a detailed investigation of their characteristic static roughening, complex dynamic behaviour, as well as direct access to the nature of the disorder potential landscape itself. Since its implementation, PFM has become the key tool for probing ferroelectric thin films, single crystals and ceramics in both fundamental and applied studies. In this technique, exploiting the piezoelectric properties inherent to all ferroelectric materials, a small oscillating bias is applied between a metallic scanning probe microscopy (SPM) tip and a planar electrode underlying the sample, and the resulting local mechanical deformation or piezoresponse measured by the vertical deflection and lateral torsion of the probe cantilever, as shown schematically in Fig. 4a. The phase of this local piezoresponse with respect to the excitation signal carries information about the polarisation orientation (see Fig. 4b), while its amplitude reflects the polarisation magnitude. For example, a full 180° phase contrast difference and a local amplitude minimum are expected across a 180° domain wall in vertical PFM imaging of an out-of-plane polarised material. While the induced piezoresponse is generally quite small (typical piezoelectric coefficients for perovskite ferroelectrics are of the order of 10–100 pm/V), lock-in amplification and resonance enhancement can significantly improve signal to noise ratios.[2]

PFM thus allows the position of individual ferroelectric domain walls to be mapped with sub-10 nm resolution over areas essentially limited only by the scan range (10s–100s μm). Moreover, novel domain-wall-specific functional properties can be readily identified, including characteristic lateral piezoresponse features in out-of-plane polarised samples [69–71], and, with additional conductive tip current measurements, domain wall electrical conduction in these otherwise insulating materials [72–76].

Beyond simply imaging, the metallic tip itself can also be used at higher bias as a nanolithographic tool to controllably switch the ferroelectric polarisation in the very local region of intense electric field generated below the tip. Artificial linear domains are thus “written” in the sample by a scanning tip held at a voltage beyond the switching threshold, while individual nanodomains are created by the application of voltage pulses to a stationary tip. Such nanodomains, whose size

[2] For a detailed review of PFM and its history, as well as the more recent advances in switching spectroscopy and band excitation techniques, we invite the reader to refer to reviews by Kalinin et al. [64,65] and Gruverman et al. [66].

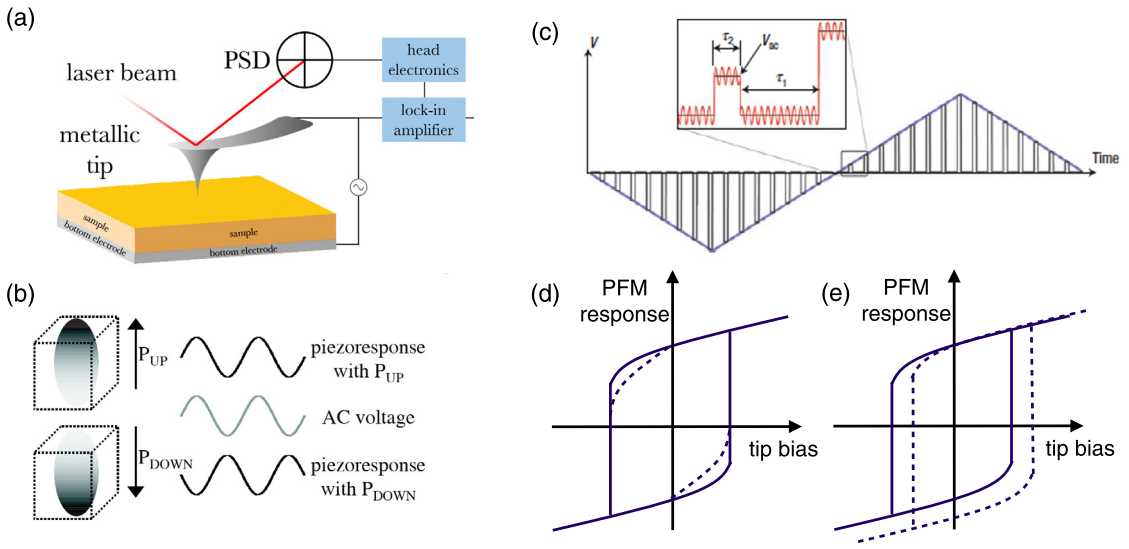

Fig. 4. Piezoresponse force microscopy (PFM). (a) A biased nanoscale metallic tip can be used to both control and probe the ferroelectric domain structure of an underlying sample. (b) Measuring the relative phase of the vertical piezoresponse with respect to the excitation signal reveals the orientation of the out-of-plane component of the ferroelectric polarisation, reproduced from [67]. (c) In switching spectroscopy–PFM (SS–PFM), a stepped triangular waveform is used to bias a stationary tip and locally measure the characteristic hysteresis of the PFM response as a result of polarisation switching, adapted from [68]. The fine structure of this response can reveal the presence of random bond (d) and random field (e) effects as rounding or imprint, respectively (dashed curve), compared to the standard hysteresis for a reference, symmetric double-well potential (solid curve), adapted from [68]. Colour available on the web.

depends on both the duration and magnitude of the voltage pulse, as well as the size of the tip itself [77,78], can be as small as a few nm in radius [79], in particular when ultrasharp tips based on carbon nanotubes are used [80–82], and remain fully stable in measurements extending over a year [83,84]. While PFM imaging is clearly neither real-time, nor full-field-of-view, information on the switching dynamics and domain growth rates in the sample can nonetheless be obtained from averaging the size of sufficient numbers of these nanodomains written with a particular voltage pulse duration and magnitude. From such measurements of domain size dependence on the writing time, which can extend over multiple decades from 1 ns to 1000 s, the domain wall velocity at a given distance from the tip can be extracted, and correlated with the electric field generated by the tip at this point [85].

A crucial step is determining the spatial distribution of this highly inhomogeneous electric field, variously considered in a point-charge or spherical approximation, or with more realistic shapes in analytical or numerical models [86,87,16,18,83,71]. Moreover, the presence of adsorbates on the ferroelectric surface can significantly influence the electric field, and screen certain types of defects, thus strongly affecting polarisation switching dynamics. In the simplest case, ferroelectric films in ambient conditions are covered by surface water, which forms a variable size, relative-humidity-dependent meniscus around the SPM tip [88,89], leading to variations in domain size [90] and in the absolute value of the coercive field [91]. Other liquids or adsorbate layers were also shown to have significant effects on the shape and growth rates of domains, with a notable transition from localised to macroscopic switching for the most conducting solvents [92,93].

Combining domain writing and imaging capabilities, PFM thus provides an extremely powerful tool to explore the fundamental static and dynamic behaviour of individual ferroelectric domain walls within the disordered elastic system framework, with an unprecedented nanoscale resolution. In addition, the more basic imaging can be coupled with switching spectroscopy piezoresponse force microscopy (SS–PFM), established by Jesse et al. [94], where the piezoresponse of a ferroelectric sample is locally probed with a stationary tip under the influence of a stepwise triangular signal, as schematically shown in Fig. 4c. This technique can probe the ferroelectric state under progressively higher electric fields, as well as the formation of transient/metastable nuclei and domain structures, and their collapse as the field is returned to zero, allowing access to the nucleation and switching dynamics over the sample surface. A combined PFM/SS–PFM approach can therefore yield direct information about the universality class of the disorder, and map the sites and activation energies for domain nucleation, reflected in the shape and fine structure of the local polarisation-tip bias hysteresis, as can be seen in Fig. 4d, e.

3.3. Nanoscale observations of roughness and creep dynamics

The first suggestion that PFM imaging could be used to access the pinning and roughening of ferroelectric domain walls came from Likodimos et al. [95,96], whose studies of triglycine sulphate single crystals showed the thermally activated growth and coarsening of intrinsic domains consistent with pinning by random impurities. Independently, following magneto-optical studies in ferromagnetic materials [97], detailed analysis of the roughness and growth of individual,

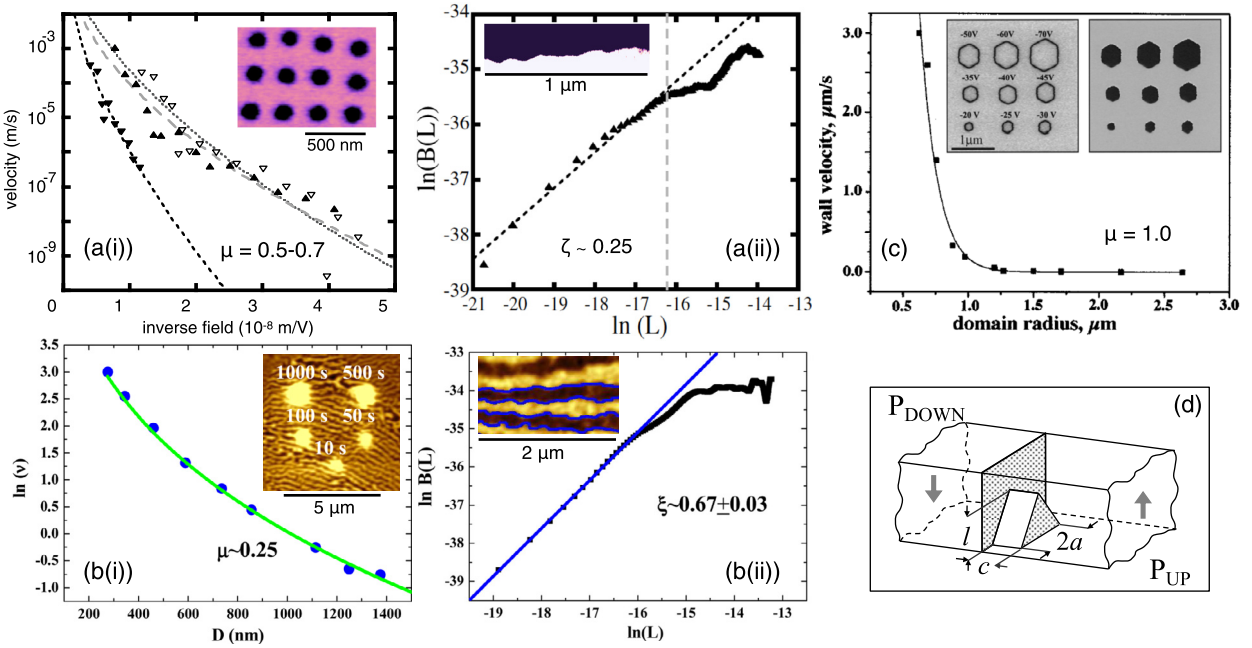

Fig. 5. Roughening and creep dynamics of ferroelectric domain walls (a(i)) Arrhenius plot of domain wall velocity in $Pb(Zr,Ti)O_3$, showing $v \sim \exp[-(1/E)^{\mu}]$ dependence on the electric field, characteristic of the creep motion of an elastic interface driven in a random pinning potential. The velocity is extracted from measurements of domain radius for arrays of domains written with a fixed duration voltage pulse, as shown in the inset. (a(ii)) Domain wall roughness of artificially-written linear domains in the same set of films, scaling as a power law of the length scale $B(r) \sim r^{2\zeta}$. (a) adapted from [98]. (b(i, ii)) Similar measurements in $(Pb,La)(Zr,Ti)O_3$ ceramic nanograins, with the roughness extracted from intrinsic domain structures, adapted from [99]. For both (a) and (b), the values of the creep and roughness exponent are compatible with random bond disorder, and 2-dimensional vs. 1-dimensional domain walls, respectively. (c) Domain growth studies in $LiNbO_3$, adapted from [100], also show creep motion, but with faceted, very regular domains (PFM amplitude and phase image in inset), consistent with pinning in the periodic lattice potential. The electric field is highly inhomogeneous, and drops off rapidly with the horizontal distance away from the biased tip $E \sim 1/r$. (d) Miller–Weinreich model of such domain wall motion via nucleation of new domains at existing domain walls, effectively moving the wall one unit cell over in the direction of domain growth, after [41]. Colour available on the web.

artificially-written domain walls in epitaxial $Pb(Zr_{0.2}Ti_{0.8})O_3$ thin films by Tybell et al., Paruch et al. [85,98,24] demonstrated non-linear creep motion at low fields, with a dynamical exponent $\mu = 0.5$–0.6, and power-law growth of the relative displacement correlation function $B(r) \sim r^{2\zeta}$ at small length scales below the ferroelectric sample thickness, with a roughness exponent $\zeta = 0.25$, as can be seen in Fig. 5a. The effective dimensionally $d_{\text{eff}} = 2.5$ was extracted using Eq. (10), in excellent agreement with theoretical predictions [31] for a two-dimensional elastic interface weakly pinned by random bond disorder, whose increased d_{eff} is due to dipolar interactions. These results opened a new area of investigation of ferroelectric materials. The very broadly applicable statistical physics approach to the effects of disorder could be used to extract universal scaling laws describing static and dynamic domain wall behaviour, and to obtain the key parameters controlling domain growth, size, and stability, important for the technological applications based on ever-smaller ferroelectric elements.

Subsequent studies largely confirmed that individual ferroelectric domain walls behave as pinned elastic interfaces, although the exact nature of the pinning potential appears to be strongly sample-dependent, with reported values of the domain wall dimensionality and creep exponent μ variously consistent with random bond disorder, random field disorder, or commensurate pinning. For example, creep dynamics were observed in domain switching studies in thinned (850 nm) $LiNbO_3$ single crystals [100], although, as for bulk samples, with extremely regular, hexagonal domains and higher values of the roughness exponent $\mu = 1$, as shown in Fig. 5c, in agreement with the Miller–Weinreich model corresponding to commensurate pinning of two-dimensional domain walls in the crystal lattice potential [41] (Fig. 5d). In combined PFM and switching current studies of domain growth in polycrystalline (150 nm) and epitaxial (100 nm) $Pb(Zr,Ti)O_3$ thin films [105,106], creep dynamics with $\mu = 0.9$–1.0 were also observed, although for the one-dimensional domain walls in these thinner films, the higher μ values appear more consistent with random field disorder, which the authors associate specifically with dipolar defects. In PFM studies of domain dynamics in relaxor ferroelectrics, $\mu = 1$ was also observed [114–116], with direct mapping of random field defects by SS–PFM [117]. In contrast, measurements of creep dynamics with $\mu = 0.5$ in epitaxial $BaTiO_3$ thin films [102], and $\mu = 0.25$ in crystallite grains extracted from $(Pb,La)(Zr,Ti)O_3$ (9.5/65/35) ceramics [99], both suggested random bond pinning, of two- and one-dimensional domain walls, respectively. In the latter study, where the roughening of intrinsic periodically ordered domains with $\zeta = 0.67$ was observed in parallel measurements (Fig. 5b), the one-dimensional nature of the domain walls was independently confirmed via layer-by-layer polishing of the sample with subsequent PFM imaging to reveal shallow disk-shaped domains formed beneath the tip. Most recently, random bond

Table 1
Analysis of ferroelectric domain walls as pinned elastic interfaces. Widely ranging values of the roughness and creep exponents were measured in different materials, as a function of the system dimensionality, of the presence of random bond, random field or correlated pinning, and of the different elastic, dipolar and strain interactions that can play a role in these systems.

Ferroelectric domain walls	ζ	μ	Ref.	Measurements
$BaTiO_3$		1.0	[42,101,41]	Switching/optical in single crystals
		0.5	[102]	PFM in thin films
TGS		1.0	[43]	Switching/optical in single crystals
		0.25	[95,96,103]	PFM in single crystals
PZT	0.2–0.3	0.5–0.8	[85,98,24]	PFM in thin films
	0.67	0.25	[99]	PFM in nanocrystallites
		0.9	[104–106]	Switching/PFM in thin films
	$0.25 \rightarrow 0.6$		[107]	PFM in thin films, T quench
	0.57	0.1–0.2	[108,109]	PFM in thin films, multiscaling
$LiTaO_3$		1.0	[110]	Switching/optical in single crystals
$LiNbO_3$		1.0	[100]	PFM in single crystals
$BiFeO_3$	0.5–0.6		[111]	PFM in thin films
	0.7–0.8		[112]	PFM in thin films, multiscaling
PVDF	0.4–0.5	0.2–0.3	[113]	PFM in thin films

Table 2
Experimental roughness and creep exponents measured in a selection of different disordered elastic systems. Once again, the wide range of values reflects different dimensionalities, pinning potentials, and interactions. In periodic systems such as flux line lattices, at large length scales interactions between the individual interfaces lead to quasi-long-range order.

System	ζ	μ	Ref.	Measurements
Ferromagnetic domain walls				
Pt.Co.Pt	0.6–0.7	0.25	[97,118]	Polarized MOKE in thin films
		0.25	[119]	Polarized MOKE in wires
	0.1	0.25	[120,121]	Polarized MOKE in thin films
Fractures				
various	∼0.8		[122]	Optical line/surface analysis
	0.4–0.6		[123–125]	Optical line/surface analysis
	0.6–0.7		[126–128]	Optical line analysis, multiscaling
Contact lines				
various	0.5		[129,130]	Optical line analysis
^4He	0.56	1.0	[131,132]	Optical line analysis
Flux line lattices				
High T_C superconductors	$0.17 \rightarrow 0$		[28,35]	Diffraction/decoration, current
	0		[133,134]	Diffraction/decoration, current
Imbibition fronts				
various	0.8		[135]	Optical line analysis
	$0.8 \rightarrow 0.6$		[136]	Optical line analysis

pinning with $\mu = 0.2$–0.3 and power-law roughening with $\zeta = 0.4$–0.5 was observed for domain walls in thin films of crystalline poly(vinylidene fluoride–trifluoroethylene) [113].

A detailed summary of the different values obtained for the roughness exponent ζ and creep exponent μ in ferroelectric materials, and their comparison with measurements in other physical systems, are presented in Table 1, and Table 2, respectively.

4. Towards more complex physics at domain walls

Although crucial in terms of determining the specifics of domain wall roughening and dynamics, the exact nature of the apparently quite heterogeneous disorder landscape was clearly difficult to access, especially in the early studies. Outside of particular cases in which the defect distribution was known, only the dominant universality class of the disorder, and not the particular type of defects or their density could be inferred from the PFM measurements. In addition, since most studies were performed on artificially-written domains, where locally very high intensity electric fields under the biased SPM tip approach dielectric breakdown limits during switching, the disorder landscape itself could be dynamically evolving during the process. These and other complex out-of-equilibrium phenomena, including ageing and memory effects, remain far less well understood. Finally, while ferroelectric domain walls, in particular in multiferroic materials, can present complex internal structure and coupled order parameters, the basic theoretical framework considers uniform, essentially structureless interfaces. Ongoing experimental and theoretical studies have begun to tackle these challenges.

4.1. The effects of a heterogeneous disorder landscape: strong pinning, dynamic disorder, and the breakdown of mono-affinity

The complex nature of the disorder landscape was for the first time directly addressed by pioneering SS–PFM studies of Jesse et al. [68], who demonstrated that in fact the disorder universality class, as determined from the shape of the local polarisation hysteresis, varied between random bond and random field over the surface of a typical $Pb(Zr,Ti)O_3$ epitaxial thin film. In addition to the random bond/random field behaviour, related to collective weak pinning by point defects, the authors also reported significant highly localised variations of the nucleation threshold across the sample. Both extended topological defects in the form of twin boundaries [68], and individual strong defects [137] were observed to pin domain walls, and to promote the nucleation of new domains, in agreement with phase field and analytical models [19]. More recently, in-situ transmission electron microscopy studies of domain nucleation and growth in ferroelectric lamellae under electric fields applied with an SPM-tip-like needle electrode directly showed the interaction between a domain wall and an individual dislocation defect [138]. Such defects, which can both spontaneously occur in epitaxial thin films as a result of substrate-induced lattice mismatch strain, and propagate into the film from substrates with lower crystalline quality, such as Verneuil-grown $SrTiO_3$, are associated with high strain gradients and elevated oxygen vacancy densities [139], thus acting as particularly strong and effective pinning sites. From all these observations, it is therefore evident that the disorder landscape in ferroelectric thin films is indeed extremely heterogeneous, and contains a wide variety of both strong and weak pinning sites, all of which interact with domain walls.

However, all the earlier studies of ferroelectric domain walls implicitly assumed weak pinning by uncorrelated disorder, with mono-affine scaling of the static equilibrium configuration fully described by the roughness $B(r)$ with a single-valued roughness exponent ζ. To determine the viability of this scenario, a more general multiscaling analysis is necessary, initially developed for studies of fracture surfaces [128]. This approach tests for potential appearance of multi-affinity, or more generally the breakdown of mono-affine scaling by direct examination of the PDF of relative displacements for any deviations from mono-affine Gaussian behaviour, and by extracting the correlation functions

$$C_n(r) = \overline{\left\langle \left| \Delta u(r) \right|^n \right\rangle}^{1/n} \sim r^{\zeta_n} \sim r^{\zeta} \tag{11}$$

These correlation functions can be collapsed to a universal curve when renormalised by the Gaussian ratios $R_n^G = C_n^G(r)/C_2^G(r)$ in the case of mono-affine scaling. For multi-affine scaling, in contrast, fanning of the renormalised displacement–displacement correlation functions indicates the different values of the ζ_n scaling exponents.

Carrying out such a multiscaling analysis of domain wall roughening for artificially-written domain structures in $Pb(Zr_{0.2}Ti_{0.8})O_3$ thin films, Guyonnet et al. [108] reported deviations from mono-affine scaling, with no collapse of the renormalised correlation functions to a universal curve. Interestingly, this behaviour appears to correlate with extremely localised features of the disorder landscape, which give rise to locally much-larger-than-average fluctuations of the relative displacement, as shown in Fig. 6a–d. Since at most one such feature was observed in each of the written domain walls, the lower bound on the crossover length beyond which mono-affine scaling appears to break down could be determined as $L_{MA} \sim 5$ μm. We note here that the Gaussian-normalised displacement–displacement correlation functions show an offset, with comparable power-law scaling for the different orders, rather than clear fanning with different exponent values, suggesting that the observed global behaviour is in fact not multi-affinity, as initially assigned, but rather the effective breakdown of correlations between segments of the domain wall separated by the localised disorder features. Indeed, considering segments of domain wall free of these localised features, mono-affine scaling is fully recovered, with a roughness exponent $\zeta = 0.57 \pm 0.06$, consistent with the roughening of one-dimensional interfaces in random bond disorder.

One possible type of defect which could give rise to such strong localised interactions with domain walls are dislocations propagating from the $SrTiO_3$ substrate, which can act as individual pinning sites [138] (see Fig. 6e). Transmission and scanning electron microscopy studies of selectively etched single crystal $SrTiO_3$ revealed dislocation densities of $\sim 10^8$ cm^{-2} [140,141], qualitatively in agreement with the observed disorder fluctuations. The ability to non-invasively identify these very localised features at the domain walls could be especially interesting when coupled with an investigation of their functional properties [74]. In particular, given that oxygen vacancies [142,143] increase domain wall conduction, and dislocation cores are associated with a very high presence of oxygen vacancies [144,139], exploring the link between multi-affinity and domain wall current levels could be a promising research pathway.

Moreover, while the theoretical framework of a pinned elastic interface generally assumes quenched disorder which does not evolve during the measurement, the defect landscape of ferroelectric thin films can be significantly altered under strong applied electric fields. Nanoscale electrodes such as the biased SPM tip, or even finer carbon nanotube wires [145, 82,83,146] used for domain switching studies produce highly inhomogeneous electric fields which can reach intensities close to dielectric breakdown, and can trigger a cascade of electrochemical effects including charge injection and relaxation dynamics, introduction and reordering of highly mobile defects such as oxygen vacancies, and even irreversible damage to the ferroelectric material [147]. These effects appear to be particularly strong at ambient conditions in the presence of surface water or other adsorbates [91,93], with very significant effects on domain size and roughening [92] even when the underlying material is not damaged or deteriorated during switching.

To further test the effects of varying disorder, Guyonnet et al. [109] also considered domain wall dynamics during switching in $Pb(Zr_{0.2}Ti_{0.8})O_3$ films grown on $SrTiO_3$ and $DyScO_3$ substrates. Epitaxial ferroelectric films grown on these two substrates show very different disorder as a result of the superior crystalline quality of Czochralski-grown $DyScO_3$, with

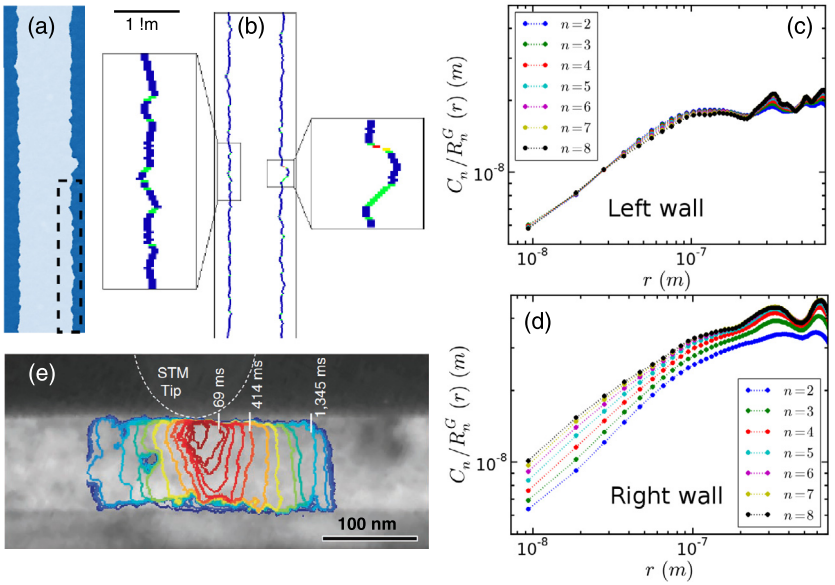

Fig. 6. The effects of individual strong pinning sites on domain wall roughness. (a) PFM image of two neighbouring domain walls in a $Pb(Zr,Ti)O_3$ thin film. For the complete length of the domain walls, the Gaussian-normalised correlation functions $C_n(r)$ show either collapse (c) or offset (d) between the different orders $n = 2$–8, indicating mono-affine roughness scaling, or its breakdown, respectively. The breakdown of mono-affinity appears to be due to strong, highly local disorder fluctuations. When such regions are excluded, for example considering only the lower part of the right wall, indicated by the dashed box, collapse of $C_n(r)$ and thus mono-affinity, is recovered. (a, c, d) Adapted from [108]. (b) Map of the local tangent slopes (absolute values) along the domain walls from (a): blue = 0.5, green = 1, yellow = 2.5, red = 3. Mono-affine segments, including the full length of the left domain wall, present only slopes $\leqslant 1$, but higher slopes can be found very locally in the regions responsible for the observed breakdown of mono-affine scaling. (e) In-situ transmission electron micrograph of domain switching in a $Pb(Zr,Ti)O_3$ thin film, showing the contours of the growing domain as a function of time, and their pinning on an individual dislocation defect, adapted from [138]. (For interpretation of the references to colour in this figure legend, the reader is referred to the web version of this article.)

significantly fewer dislocations than Verneuil-grown $SrTiO_3$, and of the high chemical activity of $SrTiO_3$ substrates during growth, leading to increased densities of oxygen vacancies [148]. Extracting domain growth dynamics from measurements of domain radius as a function of writing time in the films allows qualitatively similar creep motion to be observed in both ultrahigh vacuum and ambient conditions. However, in ultrahigh vacuum, very irregular domain shapes are seen in the presence of higher defect densities. In addition, for both low and high defect densities, very low values of the creep exponent $\mu = 0.10$–0.13 are obtained, in contrast to the ambient-condition measurements, which show $\mu = 0.15$–0.3, depending on the specific geometry of the electric field model used during fitting. Surface water thus appears to provide screening, allowing more rapid growth, and promoting rounded, uniform domains, in agreement with Landau–Ginzburg-based simulations incorporating the disorder and screening effects as random bond variations of the ferroelectric double well, and an adjustable dipolar interaction strength.

While $\mu = 0.25$ would be the expected value for the dynamical exponent governing creep motion of a one-dimensional elastic interface in random bond disorder, values of $\mu \sim 0.1$ imply extremely slow dynamics. We note, however, that strong decrease of the dynamical exponent μ was previously observed in $Pb(Zr_{0.2}Ti_{0.8})O_3$ films with extended defects, either introduced as columnar tracks following heavy ion irradiation (μ decrease from ∼0.6 to ∼0.4), or as topological defects in the form of twin walls (μ decrease from 0.5–0.7 to 0.2–0.3) [149], suggesting that lower μ values can be linked to stronger pinning. Likewise in $(Pb,La)(Zr,Ti)O_3$ ceramics with increasing disorder due to higher La densities (varying between 5–9.5 at.%), an evolution of μ values from 0.33 to 0.25 was observed [99].

4.2. Domain walls with internal structure, mixed order parameters, and out-of-equilibrium phenomena

Another area of nascent interest is in the behaviour of domain walls with complex internal structure and unusual properties within the pinned elastic interface framework. In multiferroic materials, where two or more of the ferroic orders are present, their coupling can mean that domain walls of (anti)ferromagnetic, (anti)ferroelectric and/or (anti)ferroelastic regions coincide [150–152], and would collectively negotiate the potential energy landscape. In addition, such coupling can also give rise to domain-wall-specific ferroic ordering absent from the parent material [153,154], such as the ferromagnetism which has been suggested for 109° domain walls in ferroelectric and antiferromagnetic $BiFeO_3$ [155,156]. Thus, nominally ferroelectric walls could, for example, become sensitive to magnetic impurities, and (anti)ferromagnetic walls strongly influenced by charged defects, or elastic strain. Likewise, since Bloch or Néel (anti)ferromagnetic domain walls are generally much wider (on the order of 10–100 nm) than their predominantly Ising ferroelectric counterparts (on the order of 1–10 nm) [4,23], the effective width of the coupled domain wall could be very different than that obtained from measurements of

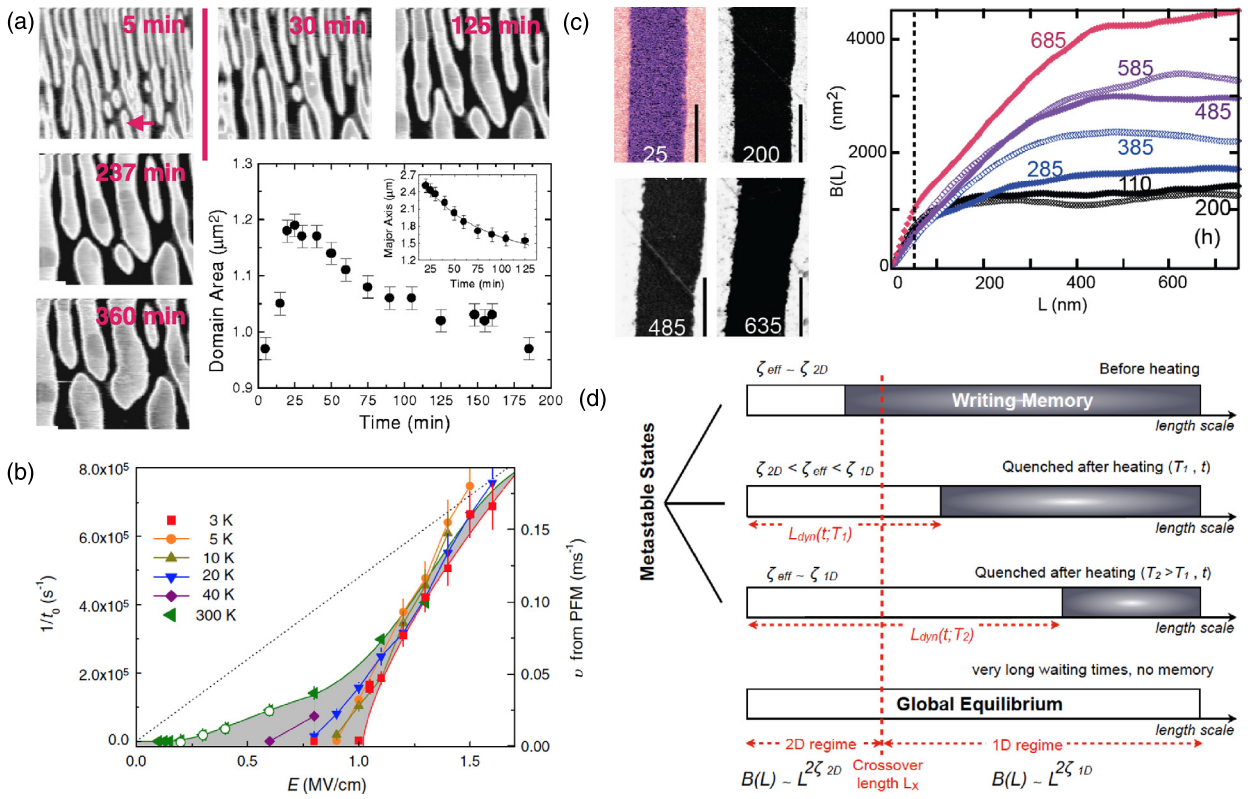

Fig. 7. Thermal effects on the roughness and dynamics of ferroelectric domain walls. (a) PFM imaging of intrinsic domains in triglycine sulphate, recorded sequentially at the indicated times at 43 °C after quenching from 60 °C. The vertical (magenta) bar corresponds to 7 μm. The temporal evolution of the area of the indicated domain allows a quantitative measurement of its coarsening. The inset shows the evolution of the major axis of the domain, with a fit to the power law $R(t) \sim (t - t_0)^{\phi}$. Adapted from [95]. (b) Temperature dependence of the inverse characteristic switching time $1/t_0$ vs. the electric field E in $Pb(Zr,Ti)O_3$ thin films, extracted from switching current measurements. Using the Komogorov–Avrami–Ishibashi expression for the time dependence of the polarisation changes $\Delta P(t) = 1 - \exp[(-t/t_0)^n]$, and assuming instantaneous nucleation, the authors relate domain wall velocity $v \sim 1/t_0$. The $1/t_0$ dependence thus appears to indicate the depinning transition, with more pronounced rounding at higher temperatures. Reproduced from [106]. (c) PFM images of the evolution of domain structures in $Pb(Zr,Ti)O_3$ thin films subjected to heating-quench cycles at progressively higher temperatures, indicated on the image. The vertical black bar corresponds to 1 μm. The domain wall roughness $B(r)$ grows after each heating-quench cycle. Whereas at lower temperatures, power-law roughness scaling is observed only at length scales $<$ the film thickness, indicated by the dashed line, after higher temperature heating-quench cycles this region extends to length scales well beyond the films thickness. Correspondingly, the roughness exponent ζ increases from 0.25 to 0.6–0.6. Adapted from [107]. (d) Schematic representation of a disorder-dominated dimensional crossover scenario compatible with the observed roughening behaviour. Before heating, the as-written, initially flat domain walls are only able to locally equilibrate at short length scales. Heating facilitates thermally activated glassy relaxation, allowing equilibration at higher length scales as the temperature increases. The fully equilibrated system is expected to show a 2D to 1D crossover at length scale $L_\times$ with no memory of the written state. Reproduced from [107]. Colour available on the web.

simply one of its order parameters, which may re-orient over a much smaller region than the other. Even in purely ferroelectric materials, complex, closure-like structures and strong interactions predicted for equilibrium periodic domain walls in very thin films [157], could also significantly increase their effective width, and potentially reduce the effects of disorder pinning, in spite of the low dimensionality of the sample.

PFM imaging studies in varying thickness $BiFeO_3$ by Catalan et al. [111] showed that the intrinsic ferroelectric domains in this material are significantly larger than those of simple ferroelectrics of comparable thickness, and closer in size to domains in magnetic materials, consistent with the strong magnetoelectric coupling at the domain walls. In addition, particularly for the thinnest films, the intrinsic domains appear extremely irregular, with mixed 71°, 109°, and 180° domain walls characterised by a fractal in-plane Hausdorff dimension of 1.4 ± 0.1, while artificially-written domains show roughness exponents of $\zeta = 0.5$–0.6. Even higher roughness exponent values of $\zeta = 0.7$–0.8 were observed by Ziegler et al. [112] for purely 71° quasi-period intrinsic domains in thicker $BiFeO_3$ films, where elastic and dipolar interactions between the domain walls, as well as strong segregation of dislocation defects related to step-bunching growth of the films [158] may be playing a role. The strong strain gradients imposed by step-bunching on vicinal miscut substrates during $BiFeO_3$ growth were shown to promote extremely directional domain wall motion under uniform electric fields applied in a planar capacitor geometry [159]. In the context of domain wall pinning, such features could act as a quasi-periodic pinning potential at length scales far larger than those of the crystal lattice of the material. These effects remain largely unexplored, both theoretically and experimentally.

Moreover, while the roughening and quasi-static slow dynamics of the domain walls can be well described within the disordered elastic system framework as the behaviour of a weakly pinned interface in equilibrium (at least at small length scales) with a random potential, much less is known about the out-of-equilibrium behaviour of such systems. From a theoretical viewpoint, understanding the non-steady slow dynamics associated with ageing [160–162] is a major challenge. An especially interesting realisation of such out-of-equilibrium phenomena is provided by quenches, in which a parameter such as temperature or the appropriate conjugate field is abruptly varied. Numerical studies of interfaces subjected to quenches [163–167] have shown ageing of the interface and a long-term memory of the initial configuration. For ferroelectrics, Likodimos et al. [95,103] studied domain evolution in cleaved triglycine sulfate crystals (Fig. 7a) subjected to annealing–cooling cycles through the transition temperature T_C, with random-bond scaling of the slow dynamics extracted from the spatial correlation functions, with a crossover to even slower behaviour. Paruch et al. [107] investigated the thermal evolution of individual domain walls following repeated heat-quench cycles up to high temperatures, but below T_C, in $Pb(Zr_{0.2}Ti_{0.8})O_3$ thin films, and found increased roughening at progressively higher length scales, with the exponent ζ changing from 0.25 to 0.5–0.6, as shown in Fig. 7c. The observed post-quench behaviour is qualitatively consistent with a locally equilibrated pinned configuration characterised by a growing dynamical length scale, whose ultra-slow evolution is primarily controlled by the defect configuration and the heating process parameters, resulting in a crossover from a two- to a one-dimensional regime, as schematically illustrated in Fig. 7d.

In addition, to investigate the role of oxygen vacancies on domain stability during the heat-quench cycling, films grown under the same conditions but cooled in process gas, pure Ar, or pure O_2 were compared. The films grown in oxygen-poor conditions, with higher densities of oxygen vacancies, showed much higher domain stability on heating, with increased roughness only at small length scales, and extensive polarisation switching only close to the Curie temperature of the films, as determined by X-ray diffraction. In these films, nanoscale circular domains could also be more easily stabilised at both ambient and high temperatures, demonstrating the crucial effects of oxygen vacancies. The stabilising effects of disorder had also been remarked for nanoscale domains written with carbon nanotubes [83], where metastable domain configurations much smaller than predicted from mean-field thermodynamic equilibrium models were followed with no evolution for over one year.

The exact behaviour of the second-order-like depinning transition is also under active theoretical investigation. Although no complete solution exists to date to the equations describing the full dynamics of the interface at finite temperature [168], advanced numerical simulations exploring thermal rounding of the dynamic response [40] have allowed accurate predictions of the depinning exponent θ for one- and two-dimensional interfaces in random bond and random field disorder. In addition, these studies suggest superroughening of the interface, with $\zeta > 1$ at depinning [169], although with nonetheless apparently mono-affine scaling. Experimentally, such anomalous scaling, previously reported in fracture surfaces [170,171], has also been extracted for ferromagnetic domain walls in ultrathin films [172]. Investigations of the crossover between creep and flow regimes [118,172] also yielded values of θ in agreement with the theoretical predictions of thermal rounding. In ferroelectrics, the early switching studies of the smallest domains in the high-field region very near the biased SPM tip allowed tentative lower bounds to be obtained for the critical electric field indicating a crossover to the faster dynamics of the depinning regime [24]. Specifically focusing on the depinning transition in measurements of switching currents from 300 K down to 3 K, Jo et al. extracted behaviour qualitatively in agreement with thermal rounding, as can be seen in Fig. 7b, although with significantly higher values of the thermal exponent θ [106]. We note that significant roughening of fast-moving ferromagnetic [173] and ferroelectric [174] domain walls was observed under high applied fields compared to a relatively smooth configuration at lower fields and velocities. In this high velocity phase, nanodomains are ejected before the advancing domain wall, whose local curvature appears to act as a precursor for the emission. A skyrmion model has been suggested to explain this process [175]. While it may be challenging to carry out high field, and variable temperature measurements, this is one area where further exploration could yield very interesting results, both theoretically and experimentally.

5. Conclusion

We have shown in this review how ferroelectric domain walls in epitaxial perovskite (multi)ferroic thin films, imaged with nanoscale resolution by PFM, provide a very useful model system for the study of the very broadly applicable physics of pinned elastic interfaces. While mono-affine roughening of the domain walls, and their ultra-slow dynamics for small applied electric fields are by now relatively well understood, far less is known about more complex aspects of the behaviour of such systems. These open questions include the effects of the extremely heterogeneous pinning landscapes present in real samples, where disorder ranging from point defects such as vacancies or substitutions to one- and two-dimensional defects in the form of threading dislocations, irradiation tracks, and twin boundaries can be introduced during or after growth. Likewise, especially in multiferroic materials, the domain walls may present complex internal structure as a result of electrostatic and strain boundary conditions, or due to the coupling of different ferroic orders, while theoretically only uniform structureless interfaces have been considered. Finally, both theoretically and experimentally, accessing out-of-equilibrium phenomena like ageing and memory effects remains a significant challenge. For all of these, ongoing studies in ferroelectric thin films have the potential to significantly increase our understanding.

Acknowledgements

The authors acknowledge close collaboration with T. Giamarchi, S. Bustingorry and A. Kolton, and thank J.-M. Triscone and D. Damjanovic for useful discussions, and S. Muller and M. Lopes for technical support. This work was partially supported by the Swiss National Science Foundation through the NCCR MaNEP. J.G. acknowledges partial support from the University of Geneva 2012 Subside Tremplin grant.

References

[1] M.E. Lines, A.M. Glass, Principles and Applications of Ferroelectrics and Related Materials, Oxford University Press, Oxford, 1977.
[2] T. Mitsui, J. Furuichi, Domain structure of Rochelle salt and KH_2PO_4, Phys. Rev. 90 (1953) 193.
[3] V.A. Zhirnov, A contribution to the theory of domain walls in ferroelectrics, Sov. Phys. JETP 35 (1959) 822.
[4] B. Meyer, D. Vanderbilt, Ab initio study of ferroelectric domain walls in $PbTiO_3$, Phys. Rev. B 65 (2002) 104111.
[5] C.-L. Jia, K.W. Urban, M. Alexe, D. Hesse, I. Vrejoiu, Direct observation of continuous electric dipole rotation in flux-closure domains in ferroelectric $Pb(Zr,Ti)O_3$, Science 331 (2011) 1420.
[6] J.F. Scott, Ferroelectric Memories, Springer, Berlin, 2000.
[7] R. Waser, A. Rüdiger, Pushing towards the digital storage limit, Nat. Mater. 3 (2004) 81.
[8] J.M. Herbert, Ferroelectric Transducers and Sensors, Gordon and Breach, New York, 1982.
[9] D. Damjanovic, P. Muralt, N. Setter, Ferroelectric sensors, IEEE Sens. J. 1 (2001) 191.
[10] A.K.S. Kumar, P. Paruch, J.M. Triscone, W. Daniau, S. Ballandras, L. Pellegrino, D. Marré, T. Tybell, High-frequency surface acoustic wave device based on thin-film piezoelectric interdigital transducers, Appl. Phys. Lett. 85 (2004) 1757.
[11] V.M. Fridkin, Photoferroelectrics, Springer-Verlag, Berlin, 1979.
[12] G. Catalan, J. Seidel, R. Ramesh, J.F. Scott, Domain wall nanoelectronics, Rev. Mod. Phys. 84 (2012) 119.
[13] E.K.H. Salje, Multiferroic boundaries as active memory devices: trajectories towards domain boundary engineering, ChemPhysChem 11 (2010) 940.
[14] H. Béa, P. Paruch, Multiferroics: a way forward along domain walls, Nat. Mater. 8 (2009) 168.
[15] S.A. Kukushkin, A.V. Osipov, Thermodynamics and kinetics of switching effects in ferroelectrics, Phys. Rev. B 65 (2002) 174101.
[16] A.N. Morozovska, E.A. Eliseev, Screening and size effects on the nanodomain tailoring in ferroelectrics semiconductors, Phys. Rev. B 73 (2006) 104440.
[17] E.A. Eliseev, A.N. Morozovska, G.S. Svechnikov, E.L. Rumyantsev, E.I. Shishkin, V.Y. Shur, S.V. Kalinin, Screening and retardation effects on 180°-domain wall motion in ferroelectrics: wall velocity and no linear dynamics due to polarisation–screening charge interactions, Phys. Rev. B 78 (2008) 245509.
[18] A.N. Morozovska, E.A. Eliseev, Y. Li, S.V. Svechnikov, P. Maksymovych, V.Y. Shur, V. Gopalan, L.-Q. Chen, S.V. Kalinin, Thermodynamics of nanodomain formation and breakdown in scanning probe microscopy: Landau–Ginzburg–Devonshire approach, Phys. Rev. B 80 (2009) 214110.
[19] A.N. Morozovska, S.V. Svechnikov, E.A. Eliseev, B.J. Rodriguez, S. Jesse, S.V. Kalinin, Local polarization switching in the presence of surface-charged defects: microscopic mechanisms and piezoresponse force spectroscopy observations, Phys. Rev. B 78 (2008) 054101.
[20] P. Mokrý, Y. Wang, A.K. Tagantsev, D. Damjanovic, I. Stolichnov, N. Setter, Evidence for dielectric aging due to progressive 180° domain wall pinning in polydomain $Pb(Zr_{0.45}Ti_{0.55})O_3$ thin films, Phys. Rev. B 79 (2009) 054104.
[21] S. Pöykkö, D.J. Chadi, Ab initio study of 180° domain wall energy and structure in $PbTiO_3$, Appl. Phys. Lett. 75 (1999) 2830.
[22] L. He, D. Vanderbilt, First-principles study of oxygen-vacancy pinning of domain walls in $PbTiO_3$, Phys. Rev. B 68 (2003) 134103.
[23] D. Lee, R.K. Behera, P. Wu, H. Xu, Y.L. Li, S.B. Sinnott, W.R. Phillpot, L.Q. Chen, V. Gopalan, Mixed Bloch–Neel–Ising character of 180° ferroelectric domain walls, Phys. Rev. B 80 (2009) 060102.
[24] P. Paruch, T. Giamarchi, T. Tybell, J.-M. Triscone, Nanoscale studies of domain wall motion in epitaxial ferroelectric thin films, J. Appl. Phys. 100 (2006) 051608.
[25] T. Giamarchi, A.B. Kolton, A. Rosso, Dynamics of disordered elastic systems, in: M.C. Miguel, J.M. Rubi (Eds.), Jamming, Yielding and Irreversible Deformation in Condensed Matter, Springer-Verlag, Berlin, 2006, p. 91, arXiv:cond-mat/0503437.
[26] P. Paruch, T. Giamarchi, J.-M. Triscone, Nanoscale Studies of Domain Walls in Epitaxial Ferroelectric Thin Films, Springer, Berlin/Heidelberg, 2007, arXiv:cond-mat/0503437.
[27] A.-L. Barabasi, H.E. Stanley, Fractal Concepts in Surface Growth, Cambridge University Press, New York, 1995.
[28] G. Blatter, M.V. Feigel'man, V.B. Geshkenbein, A.I. Larkin, V.M. Vinokur, Vortices in high-temperature superconductors, Rev. Mod. Phys. 66 (1994) 1125.
[29] E. Agoritsas, V. Lecomte, T. Giamarchi, Disordered elastic systems and one-dimensional interfaces, Physica B 407 (2012) 1725.
[30] E. Agoritsas, S. Bustingorry, V. Lecomte, G. Schehr, T. Giamarchi, Finite-temperature and finite-time scaling of the directed polymer free-energy with respect to its geometrical fluctuations, Phys. Rev. E 86 (2012) 031144.
[31] T. Nattermann, Interface phenomenology, dipolar interaction, and the dimensionality dependence of the incommensurate–commensurate transition, J. Phys. C 16 (1983) 4125.
[32] T. Emig, T. Nattermann, Disorder driven roughening transitions of elastic manifolds and periodic elastic media, Eur. Phys. J. B 8 (1999) 525.
[33] L. Landau, E. Lifshitz, Theory of the dispersion of magnetic permeability in ferromagnetic bodies, Z. Phys. Sov. 8 (1935) 153.
[34] C. Kittel, Theory of the structure of ferromagnetic domains in films and small particles, Phys. Rev. 70 (1946) 965.
[35] T. Giamarchi, S. Bhattacharya, Vortex phases, in: Claude Berthier, Laurent P. Levy, Gerard Martinez (Eds.), High Magnetic Fields: Applications in Condensed Matter Physics and Spectroscopy, Springer-Verlag, Berlin, 2002, p. 314, arXiv:cond-mat/0111052.
[36] T. Halpin-Healy, Directed polymers in random media probability distributions, Phys. Rev. A 44 (1991) R3415.
[37] M. Mézard, G. Parisi, Replica field theory for random manifolds, J. Phys. I 1 (1991) 809.
[38] A. Rosso, R. Santachiara, W. Krauth, Geometry of Gaussian signals, J. Stat. Mech. Theory Exp. (2005) L08001.
[39] A.-L. Barabasi, R. Bourbonnais, M. Jensen, J. Kertesz, T. Vicsek, Y.-C. Zhang, Multifractality of growing surfaces, Phys. Rev. A 45 (1992) R6951.
[40] S. Bustingorry, A.B. Kolton, T. Giamarchi, Thermal rounding of the depinning transition, Europhys. Lett. 81 (2008) 26005.
[41] R.C. Miller, G. Weinreich, Mechanism for the sidewise motion of 180° domain walls in barium titanate, Phys. Rev. 117 (1960) 1460.
[42] W.J. Merz, Domain formation and domain wall motions in ferroelectric $BaTiO_3$ single crystals, Phys. Rev. 95 (1954) 690.
[43] F. Fatuzzo, W.J. Merz, Switching mechanism in triglycine sulfate and other ferroelectrics, Phys. Rev. 116 (1959) 61.
[44] Y.-H. Shin, I. Grinberg, I.-W. Chen, A.M. Rappe, Nucleation and growth mechanism of ferroelectric domain-wall motion, Nature 449 (2007) 881.
[45] Y. Ishibashi, Y. Takagi, Note on ferroelectric domain switching, J. Phys. Soc. Jpn. 31 (1971) 506.
[46] Y. Ishibashi, Polarization Reversals in Ferroelectrics, Gordon and Breach, Amsterdam, 1996.
[47] V.Y. Shur, Fast Polarisation Reversal Process: Evolution of Ferroelectric Domain Structure in Thin Films, Gordon and Breach, Amsterdam, 1996.
[48] T. Natterman, T. Emig, A new disorder-driven roughening transition of charge-density waves and flux-line lattices, Phys. Rev. Lett. 79 (1997) 5090.
[49] T. Nattermann, Interface roughening in systems with quenched random impurities, Europhys. Lett. 4 (1987) 1241.
[50] T. Nattermann, Y. Shapir, I. Vilfan, Interface pinning and dynamics in random systems, Phys. Rev. B 42 (1990) 8577.
[51] D. Damjanovic, Ferroelectric, dielectric and piezoelectric properties of ferroelectric thin films and ceramics, Rep. Prog. Phys. 61 (1998) 1267.

[52] D.V. Taylor, D. Damjanovic, Evidence of domain wall contribution to the dielectric permittivity in PZT thin films at sub-switching fields, J. Appl. Phys. 82 (1997) 1973.
[53] D.V. Taylor, D. Damjanovic, Domain wall pinning contribution to the nonlinear dielectric permittivity in Pb(Zr,Ti)O_3 thin films, Appl. Phys. Lett. 73 (1998) 2045.
[54] D. Damjanovic, Logarithmic frequency dependence of the piezoelectric effect due to pinning of ferroelectric–ferroelastic domain walls, Phys. Rev. B 55 (1997) R649.
[55] D. Damjanovic, Stress and frequency dependence of the direct piezoelectric effect in ferroelectric ceramics, J. Appl. Phys. 82 (1997) 1788.
[56] W. Kleemann, P. Licinio, T. Woike, R. Pankrath, Dynamic light scattering at domains and nano clusters in a relaxor ferroelectric, Phys. Rev. Lett. 86 (2001) 220101.
[57] V. Mueller, Y. Shchur, H. Beige, S. Mattauch, J. Glinnemann, G. Heger, Non-Debye domain wall response in KH_2PO_4, Phys. Rev. B 65 (2002) 134102.
[58] J. Banys, J. Macutkevic, R. Grigalaitis, W. Kleemann, Dynamics of nanoscale polar regions and critical behavior of the uniaxial relaxor $Sr_{0.61}Ba_{0.39}Nb_2O_6$:Co, Phys. Rev. B 72 (2005) 024106.
[59] W. Kleemann, J. Dec, S. Miga, R. Pankrath, Non-Debye domain-wall-induced dielectric response in $Sr_{0.61-x}Ce_xBa_{0.39}Nb_2O_6$, Phys. Rev. B 65 (2002) 220101.
[60] D.R. Taylor, J.T. Love, G.J. Topping, J.G.A. Dane, Crossover from pure to random-field critical susceptibility in $KH_2As_xP_{1-x}O_4$, Phys. Rev. B 72 (2005) 052109.
[61] W. Kleemann, Universal domain wall dynamics in disordered ferroic materials, Annu. Rev. Mater. Res. 37 (2007) 415.
[62] T. Braun, W. Kleeman, J. Dec, P.A. Thomas, Creep and relaxation dynamics of domain walls in periodically poled $KTiOPO_4$, Phys. Rev. Lett. 94 (2005) 117601.
[63] T.J. Yang, V. Gopalan, P.J. Swart, U. Mohadeen, Direct observation of pinning and bowing of a single ferroelectric domain wall, Phys. Rev. Lett. 82 (1999) 4106.
[64] S.V. Kalinin, B.J. Rodriguez, S. Jesse, J. Shin, A.P. Baddorf, P. Gupta, H. Jain, D.B. Williams, A. Gruverman, Vector piezoresponse force microscopy, Microsc. Microanal. 12 (2006) 206.
[65] S.V. Kalinin, A.N. Morozovska, L.Q. Chen, B.J. Rodriguez, Local polarization dynamics in ferroelectric materials, Rep. Prog. Phys. 73 (2010) 056502.
[66] A. Gruverman, S.V. Kalinin, Piezoresponse force microscopy and recent advances in nanoscale studies of ferroelectrics, J. Mater. Sci. 41 (2006) 107.
[67] P. Paruch, Atomic force microscopy studies of ferroelectric domain in epitaxial $PbZr_{0.2}Ti_{0.8}O_3$ thin films and the static and dynamic behaviour of ferroelectric domain walls, PhD thesis, 2004.
[68] S. Jesse, B.J. Rodriguez, S. Choudhury, A.P. Baddorf, I. Vrejoiu, D. Hesse, M. Alexe, E.A. Eliseev, A.N. Morozovska, J. Zhang, L.-Q. Chen, S.V. Kalinin, Direct imaging of the spatial and energy distribution of nucleation centres in ferroelectric materials, Nat. Mater. 7 (2008) 209.
[69] J. Guyonnet, H. Béa, F. Guy, S. Gariglio, S. Fusil, K. Bouzehouane, J.-M. Triscone, P. Paruch, Shear effects in lateral piezoresponse force microscopy at 180° ferroelectric domain walls, Appl. Phys. Lett. 95 (2009) 132902.
[70] J. Guyonnet, H. Béa, P. Paruch, Lateral piezoresponse across ferroelectric domain walls in thin films, J. Appl. Phys. 108 (2010) 042002.
[71] S. Lei, E.A. Eliseev, A.N. Morozovska, R.C. Haislmeier, T.T.A. Lummen, W. Cao, S.V. Kalinin, V. Gopalan, Origin of piezoelectric response under a biased scanning probe microscopy tip across a 180° ferroelectric domain wall, Phys. Rev. B 86 (2012) 134115.
[72] J. Seidel, L.W. Martin, Q. He, Q. Zhan, Y.-H. Chu, A. Rother, M.E. Hawkridge, P. Maksymovych, P. Yu, M. Gajek, N. Balke, S.V. Kalinin, S. Gemming, F. Want, G. Catalan, J.F. Scott, N.A. Spaldin, J. Orenstein, R. Ramesh, Conduction at domain walls in oxide multiferroics, Nat. Mater. 8 (2009) 229.
[73] S. Farokhipoor, B. Noheda, Conduction through 71° domain walls in $BiFeO_3$ thin films, Phys. Rev. Lett. 107 (2011) 127601.
[74] J. Guyonnet, I. Gaponenko, S. Gariglio, P. Paruch, Conduction at domain walls in insulating $Pb(Zr_{0.2}Ti_{0.8})O_3$ thin films, Adv. Mater. 23 (2011) 5377.
[75] W. Wu, Y. Horibe, N. Lee, S.-W. Cheong, J.R. Guest, Conduction of topologically protected charged ferroelectric domain walls, Phys. Rev. Lett. 108 (2012) 077203.
[76] D. Meier, A. Cano, K. Delaney, Y. Kumagai, M. Mostovoy, N.A. Spaldin, R. Ramesh, M. Fiebig, Anisotropic conductance at improper ferroelectric domain walls, Nat. Mater. 11 (2012) 284.
[77] P. Paruch, T. Tybell, J.-M. Triscone, Nanoscale control of ferroelectric polarization and domain size in epitaxial $Pb(Zr_{0.2}Ti_{0.8})O_3$ thin films, Appl. Phys. Lett. 79 (2001) 530.
[78] K. Terabe, M. Nakamura, S. Takekawa, K. Kitamura, S. Higuchi, Y. Gotoh, Y. Cho, Microscale to nanoscale ferroelectric domain and surface engineering of a near stoichiometric $LiNbO_3$ film, Appl. Phys. Lett. 82 (2003) 433.
[79] Y. Cho, K. Fujimoto, Y. Hiranaga, Y. Wagatsuma, A. Onoe, K. Terabe, K. Kitamura, Tbit/inch^2 ferroelectric data storage based on scanning nonlinear dielectric microscopy, Appl. Phys. Lett. 81 (2002) 4401.
[80] P. Paruch, T. Tybell, J.-M. Triscone, Nanoscale control and domain wall dynamics in epitaxial ferroelectric $Pb(Zr_{0.2}Ti_{0.8})O_3$ thin films, in: Proc. 10th Int. Ceram. Cong. CIMTEC 2002 D, 2002, p. 675.
[81] N. Tayebi, Y. Narui, R.J. Chen, C.P. Collier, K.P. Giapis, Y. Zhang, Nanopencil as a wear-tolerant probe for ultrahigh density data storage, Appl. Phys. Lett. 93 (2008) 103112.
[82] N. Tayebi, Y. Narui, N. Franklin, C.P. Collier, K.P. Giapis, Y. Nishi, Y. Zhang, Fully inverted single-digit nanometer domains in ferroelectric films, Appl. Phys. Lett. 96 (2010) 023103.
[83] C. Blaser, P. Paruch, Minimum domain size and stability in carbon nanotube-ferroelectric devices, Appl. Phys. Lett. 101 (2012) 142906.
[84] T. Maruyama, M. Saitoh, I. Sakai, T. Hidaka, Y. Yano, T. Noguchi, Growth and characterization of 10-nm-thick *c*-axis oriented epitaxial $PbZr_{0.25}Ti_{0.75}O_3$ thin films on (100)Si substrate, Appl. Phys. Lett. 73 (1998) 3524.
[85] T. Tybell, P. Paruch, T. Giamarchi, J.-M. Triscone, Domain wall creep in epitaxial ferroelectric $PbZr_{0.2}Ti_{0.8}O_3$ thin films, Phys. Rev. Lett. 89 (2002) 097601.
[86] S.V. Kalinin, D.A. Bonnell, Imaging mechanism of piezoresponse force microscopy of ferroelectric surfaces, Phys. Rev. B 65 (2002) 125408.
[87] M. Molotskii, Generation of ferroelectric domains in atomic force microscope, J. Appl. Phys. 93 (2003) 6234.
[88] B.L. Weeks, M.W. Vaughn, J.J. DeYoreo, Direct imaging of meniscus formation in atomic force microscopy using environmental scanning electron microscopy, Langmuir 21 (2005) 8096.
[89] B.J. Rodriguez, S. Jesse, A.P. Baddorf, S.V. Kalinin, High resolution electromechanical imaging of ferroelectric materials in a liquid environment by piezoresponse force microscopy, Phys. Rev. Lett. 96 (2006) 237602.
[90] D. Dahan, M. Molotskii, G. Rosenman, Y. Rosenwaks, Ferroelectric domain inversion: the role of humidity, Appl. Phys. Lett. 89 (2006) 152902.
[91] P. Maksymovych, S. Jesse, M. Hujiben, R. Ramehs, A. Morozovska, S. Choudhury, L.-Q. Chen, A.P. Baddorf, S.V. Kalinin, Intrinsic nucleation mechanism and disorder effects in polarization switching on ferroelectric surfaces, Phys. Rev. Lett. 102 (2009) 017601.
[92] B.J. Rodriguez, S. Jesse, A.P. Baddorf, S.-H. Kim, S.V. Kalinin, Controlling polarization dynamics in a liquid environment: from localized to macroscopic switching in ferroelectrics, Phys. Rev. Lett. 98 (2007) 247603.
[93] V.Y. Shur, A.V. Ievlev, E.V. Nikolaeva, E.I. Shishkin, M.M. Neradovsky, Influence of adsorbed surface layer on domain growth in the field produced by conductive tip of scanning probe microscope in lithium niobate, J. Appl. Phys. 110 (2011) 052017.
[94] S. Jesse, A.P. Baddorf, S.V. Kalinin, Switching spectroscopy piezoresponse force microscopy of ferroelectric materials, Appl. Phys. Lett. 88 (2006) 062908.
[95] V. Likodimos, M. Labardi, M. Allegrini, Kinetics of ferroelectric domains investigated by scanning force microscopy, Phys. Rev. B 61 (2000) 14440.

[96] V. Likodimos, M. Labardi, X.K. Orlik, L. Pardi, M. Allegrini, Thermally activated ferroelectric domain growth due to random defects, Phys. Rev. B 63 (2001) 064104.
[97] S. Lemerle, J. Ferré, C. Chappert, V. Mathet, T. Giamarchi, P. Le Doussal, Domain wall creep in an Ising ultrathin magnetic film, Phys. Rev. Lett. 80 (1998) 849.
[98] P. Paruch, T. Giamarchi, J.-M. Triscone, Domain wall roughness in epitaxial ferroelectric $PbZr_{0.2}Ti_{0.8}O_3$ thin films, Phys. Rev. Lett. 94 (2005) 197601.
[99] N.A. Pertsev, D.A. Kiselev, I.K. Bdikin, M. Kosec, A.L. Kholkin, Quasi-one-dimensional domain walls in ferroelectric ceramics: Evidence from domain dynamics and wall roughness measurements, J. Appl. Phys. 110 (2011) 052001.
[100] B.J. Rodriguez, A.J. Nemanich, A. Kingon, A. Gruverman, S.V. Kalinin, K. Terabe, X.Y. Liu, K. Kitamura, Domain growth kinetics in lithium niobate single crystals studied by piezoresponse force microscopy, Appl. Phys. Lett. 86 (2005) 012906.
[101] R.C. Miller, A. Savage, Further experiments on the sidewise motion of 180° domain walls in $BaTiO_3$, Phys. Rev. 115 (1959) 1460.
[102] N.A. Pertsev, A. Petraru, H. Kohlstedt, R. Waser, I.K. Bdikin, D.A. Kiselev, A.L. Kholkin, Dynamics of ferroelectric nanodomains in $BaTiO_3$ epitaxial thin films via piezoresponse force microscopy, Nanotechnology 19 (2008) 375703.
[103] V. Likodimos, M. Labardi, M. Allegrini, Domain pattern formation and kinetics on ferroelectric surfaces under thermal cycling using scanning force microscopy, Phys. Rev. B 66 (2002) 024104.
[104] J.Y. Jo, D.K. Kim, Y.S. Kim, S.-B. Choe, T.K. Song, J.-G. Yoon, T.W. Noh, Polarization switching dynamics governed by the thermodynamic nucleation process in ultrathin ferroelectric films, Phys. Rev. Lett. 97 (2006) 247602.
[105] J.Y. Jo, H.S. Han, J.-G. Yoon, T.K. Song, S.-H. Kim, T.W. Noh, Domain switching kinetics in disordered ferroelectric thin films, Phys. Rev. Lett. 99 (2007) 267602.
[106] J.Y. Jo, S.M. Yang, T.H. Kim, H.N. Lee, J.-G. Yoon, S. Park, Y. Jo, M.H. Jung, T.W. Noh, Nonlinear dynamics of domain-wall propagation in epitaxial ferroelectric thin films, Phys. Rev. Lett. 102 (2009) 045701.
[107] P. Paruch, A.B. Kolton, X. Hong, C.H. Ahn, T. Giamarchi, Thermal quench effects on ferroelectric domain walls, Phys. Rev. B 85 (2012) 214115.
[108] J. Guyonnet, E. Agoritsas, S. Bustingorry, T. Giamarchi, P. Paruch, Multiscaling analysis of ferroelectric domain wall roughness, Phys. Rev. Lett. 109 (2012) 147601.
[109] J. Guyonnet, S. Bustingorry, C. Blaser, E.E. Ferrero, I. Gaponenko, J. Karthik, L.W. Martin, P. Paruch, Assessment of environmental and disorder effects on ferroelectric domain dynamics, Phys. Rev. Lett. (2013), submitted for publication.
[110] V.Y. Shur, E.V. Nikolaeva, E.I. Shishkin, V.L. Kozhevnikov, A.P. Chernykh, K. Terabe, K. Kitamura, Polarization reversal in congruent and stoichiometric lithium tantalate, Appl. Phys. Lett. 79 (2001) 3146.
[111] G. Catalan, H. Béa, S. Fusil, M. Bibes, P. Paruch, A. Barthélémy, J.F. Scott, Fractal dimension and size scaling of domains in thin films of multiferroic $BiFeO_3$, Phys. Rev. Lett. 100 (2008) 027602.
[112] B. Ziegler, K. Martens, T. Giamarchi, P. Paruch, Domain wall roughness in the stripe phase of $BiFeO_3$ thin films, Phys. Rev. Lett. (2013), submitted for publication.
[113] Z. Xiao, S. Poddar, S. Ducharme, X. Hong, Domain wall roughness and creep in nanoscale crystalline ferroelectric polymer, Appl. Phys. Lett. (2013), in press.
[114] V.V. Shvartsman, B. Dhkil, A.L. Kholkin, Mesoscale domains and nature of the relaxor state by piezoresponse force microscopy, Annu. Rev. Mater. Res. 43 (2013).
[115] T.R. Volk, L.V. Simagina, R.V. Gainutdinov, A.L. Tolstikhina, L.I. Ivleva, Ferroelectric micro domains and micro domain arrays recorder in strontium–barium niobate crystals in the field of atomic force microscope, J. Appl. Phys. 108 (2010) 042010.
[116] T.R. Volk, L.V. Simagina, R.V. Gainutdinov, E.S. Ivanova, L.I. Ivleva, S.V. Mit'ko, Scanning probe microscopy investigation of ferroelectric properties of barium strontium niobate crystals, Phys. Solid State 53 (2011) 2468.
[117] B.J. Rodriguez, S. Jesse, A.A. Bokov, Z.-G. Ye, S.V. Kalinin, Mapping bias-induced phase stability and random fields in relaxor ferroelectrics, Appl. Phys. Lett. 95 (2009) 092904.
[118] W.J. Metaxas, J.P. Jamet, A. Mougin, M. Cormier, J. Ferré, V. Baltz, B. Rodmacq, B. Dieny, R.L. Stamps, Creep and flow regimes of magnetic domain-wall motion in ultrathin Pt/Co/Pt films with perpendicular anisotropy, Phys. Rev. Lett. 99 (2007) 217208.
[119] F. Cayssol, D. Ravelosona, C. Chappert, J. Ferré, J.P. Jamet, Domain wall creep in magnetic wires, Phys. Rev. Lett. 92 (2004) 107202.
[120] L. Krusin-Elbaum, T. Shibauchi, B. Argyle, L. Gignac, Stable ultrahigh-density magneto-optical recordings using introduced linear defects, Nature 410 (2001) 444.
[121] T. Shibauchi, L. Krusin-Elbaum, V.M. Vinokur, B. Argyle, D. Weller, B.D. Terris, Deroughening of a 1D domain wall in an ultrathin magnetic film by a correlated defect, Phys. Rev. Lett. 87 (2001) 267201.
[122] E. Bouchaud, Scaling properties of cracks, J. Phys. Condens. Matter 9 (1997) 4319.
[123] J.M. Boffa, C. Allain, J.P. Hulin, Experimental analysis of fracture rugosity in granular and compact rocks, Eur. Phys. J. Appl. Phys. 2 (1997) 281.
[124] L. Ponson, D. Bonamy, E. Bouchaud, Two-dimensional scaling properties of experimental fracture surfaces, Phys. Rev. Lett. 96 (2006) 035506.
[125] D. Bonamy, L. Ponson, S. Prades, E. Bouchaud, C. Guillot, Scaling exponents for fracture surfaces in homogeneous glass and glassy ceramics, Phys. Rev. Lett. 97 (2006) 135504.
[126] M.J. Alava, P.K.V.V. Nukala, S. Zapperi, Morphology of two-dimensional fracture surfaces, J. Stat. Mech. Theory Exp. (2006) L10002.
[127] E. Bouchbinder, I. Procaccia, S. Santucci, L. Vanel, Fracture surfaces as multiscaling graphs, Phys. Rev. Lett. 96 (2006) 055509.
[128] S. Santucci, K.J. Måløy, A. Delaplace, J. Mathiesen, A. Hansen, J.O.H. Bakke, J. Schmittbuhl, L. Vanel, R. Purusattam, Statistics of fracture surfaces, Phys. Rev. E 75 (2007) 016104.
[129] S. Moulinet, C. Guthmann, E. Rolley, Roughness and dynamics of a contact line of a viscous fluid on a disordered substrate, Eur. Phys. J. E 8 (2002) 437.
[130] S. Moulinet, A. Rosso, W. Krauth, E. Rolley, Width distribution of contact lines on a disordered substrate, Phys. Rev. E 69 (2004) 35103.
[131] A. Prevost, E. Rolley, C. Guthmann, Thermally activated motion of the contact line of a liquid ^{4}He meniscus on a cesium substrate, Phys. Rev. Lett. 83 (1999) 348.
[132] A. Prevost, E. Rolley, C. Guthmann, Dynamics of a helium-4 meniscus on a strongly disordered cesium substrate, Phys. Rev. B 65 (2002) 04517.
[133] D.T. Fuchs, E. Zeldov, T. Tamegai, S. Ooi, M. Rappaport, H. Shtrikman, Possible new vortex matter phases in $Bi_2Sr_2CaCu_2O_8$, Phys. Rev. Lett. 80 (1998) 4971.
[134] C.J. van der Beek, S. Colson, M. Konczykowski, M.V. Indenbom, R.J. Drost, P.H. Kes, Magnetic relaxation in the "Bragg-glass" phase in BSCCO, Physica C 341–348 (2000) 1279.
[135] V.K. Horváth, F. Family, T. Vicsek, Anomalous noise distribution of the interface in two-phase fluid flow, Phys. Rev. Lett. 67 (1991) 3207.
[136] D. Geromichalos, F. Mugele, S. Hrminghaus, Nonlocal dynamics of spontaneous imbibition fronts, Phys. Rev. Lett. 89 (2002) 104503.
[137] S.V. Kalinin, S. Jesse, B.J. Rodriguez, Y.H. Chu, R. Ramesh, E.A. Eliseev, A.N. Morozovska, Probing the role of single defects on the thermodynamics of electric-field induced phase transitions, Phys. Rev. Lett. 100 (2008) 155703.
[138] P. Gao, C.T. Nelson, J.R. Jokisaari, S.-H. Baek, C.W. Bark, Y. Zhang, E. Wang, D.G. Schlom, C.-B. Eom, X. Pan, Revealing the role of defects in ferroelectric switching with atomic resolution, Nat. Commun. 2 (2011) 591.
[139] K. Szot, W. Speier, G. Bihlmayer, R. Waser, Switching the electrical resistance of individual dislocations in single-crystalline $SrTiO_3$, Nat. Mater. 5 (2006) 312.

[140] R. Wang, Y. Zhu, S.M. Shapiro, Structural defects and the origin of the second length scale in $SrTiO_3$, Phys. Rev. Lett. 80 (1998) 2370.
[141] R.J. Kamaladasa, W. Jiang, Y.N. Picard, Imaging dislocations in single-crystal $SrTiO_3$ substrates by electron channeling, J. Electron. Mater. 40 (2011) 2222.
[142] J. Seidel, P.M.Y. Batra, A. Katan, S.-Y. Yang, Q. He, A.P. Baddorf, S.V. Kalinin, C.-H. Yang, J.-C. Yang, Y.-H. Chu, E.K.H. Salje, H. Wromeester, M. Salmeron, R. Ramesh, Domain wall conductivity in La-doped $BiFeO_3$, Phys. Rev. Lett. 105 (2010) 197603.
[143] S. Farokhipoor, B. Noheda, Local conductivity and the role of vacancies around twin walls of (001)-$BiFeO_3$ thin films, J. Appl. Phys. 112 (2012) 052003.
[144] C.-L. Jia, A. Thust, K.W. Urban, Atomic-scale analysis of the oxygen configuration at a $SrTiO_3$ dislocation core, Phys. Rev. Lett. 95 (2005) 225506.
[145] P. Paruch, A.-B. Posadas, M. Dawber, C.H. Ahn, P.L. McEuen, Polarization switching using single-walled carbon nanotubes grown on epitaxial ferroelectric thin films, Appl. Phys. Lett. 93 (2008) 132901.
[146] C. Blaser, V. Esposito, P. Paruch, Understanding polarization vs. charge dynamics effects in ferroelectric-carbon nanotube devices, Appl. Phys. Lett. 102 (2013) 223503.
[147] S.V. Kalinin, S. Jesse, A. Tselev, A.P. Baddorf, N. Balke, The role of electrochemical phenomena in scanning probe microscopy of ferroelectric thin films, ACS Nano 5 (2011) 5683.
[148] G.L. Yuan, L.W. Martin, R. Ramesh, A. Uedono, The dependence of oxygen vacancy distributions in $BiFeO_3$ films on oxygen pressure and substrate, Appl. Phys. Lett. 95 (2009) 012904.
[149] P. Paruch, T. Giamarchi, J.-M. Triscone, Domain wall creep in mixed c–a axis $Pb(Zr_{0.2}Ti_{0.8})O_3$ thin films, Ann. Phys. 13 (2004) 95.
[150] M. Fiebig, T. Lottermoser, D. Frölich, A.V. Goltsev, R.V. Pisarev, Observation of coupled magnetic and electric domains, Nature 419 (2002) 818.
[151] C. Ederer, N.A. Spaldin, Magnetoelectrics – a new route to magnetic ferroelectrics, Nat. Mater. 3 (2004) 849.
[152] Y. Chu, L.W. Martin, M.B. Holcomb, M. Gajek, S.-J. Han, Q. He, N. Balke, C.-H. Yang, D. Lee, W. Hu, Q. Zhan, P.-L. Yang, A. Fraile-Rodriguez, A. Scholl, S. Wang, R. Ramesh, Electric-field control of local ferromagnetism using a magnetoelectric multiferroic, Nat. Mater. 7 (2010) 478.
[153] B. Houchmandzadeh, J. Lajzerowicz, E. Salje, Order parameter coupling and chirality of domain walls, J. Phys. Condens. Matter 3 (1991) 5163.
[154] M. Daraktchiev, G. Catalan, J.F. Scott, Landau theory of domain wall magnetoelectricity, Phys. Rev. B 81 (2010) 224118.
[155] L.W. Martin, Y.-H. Chu, M. Holcomb, M. Hujiben, P. Yu, S.-J. Han, D. Lee, S.X. Wang, R. Ramesh, Nanoscale control of exchange bias with $BiFeO_3$ thin films, Nano Lett. 8 (2008) 2050.
[156] G. Catalan, J.F. Scott, Physics and applications of bismuth ferrite, Adv. Mater. 21 (2009) 2463.
[157] P. Aguado-Puente, J. Junquera, Ferromagneticlike closure domains in ferroelectric ultrathin films: first-principles simulations, Phys. Rev. Lett. 100 (2008) 177601.
[158] T.H. Kim, S.H. Baek, S.Y. Jang, S.M. Yang, S.H. Chang, T.K. Song, J.-G. Yoon, C.B. Eom, J.-S. Chung, T.W. Noh, Step bunching-induced vertical lattice mismatch and crystallographic tilt in vicinal $BiFeO_3$(001) films, Appl. Phys. Lett. 98 (2011) 022904.
[159] T.H. Kim, S.H. Baek, S.M. Yang, S.Y. Jang, D. Ortiz, T.K. Song, J.-S. Chung, C.B. Eom, T.W. Noh, J.-G. Yoon, Electric-field-controlled directional motion of ferroelectric domain walls in multiferroic $BiFeO_3$ films, Appl. Phys. Lett. 95 (2009) 262902.
[160] J.P. Bouchaud, L.F. Cugliandolo, J. Kurchan, M. Mezard, Out of Equilibrium Dynamics in Spin-Glasses and Other Glassy Systems, World Scientific, Singapore, 1998.
[161] L.F. Cugliandolo, T. Giamarchi, P. Le Doussal, Dynamic compressibility and aging in Wigner crystals and quantum glasses, Phys. Rev. Lett. 96 (2006) 217203.
[162] G. Schehr, P.L. Doussal, Functional renormalization for pinned elastic systems away from their steady states, Europhys. Lett. 71 (2005) 290.
[163] A.B. Kolton, A. Rosso, T. Giamarchi, Relaxation of a flat interface, Phys. Rev. Lett. 95 (2005) 180604.
[164] S. Bustingorry, L.F. Cugliandolo, D. Dominguez, Langevin simulations of the out-of-equilibrium dynamics of the vortex glass in high-temperature superconductors, Phys. Rev. B 75 (2007) 024506.
[165] J.L. Iguain, S. Bustingorry, A.B. Kolton, L.F. Cugliandolo, Growing correlations and aging of an elastic line in a random potential, Phys. Rev. B 80 (2009) 094201.
[166] A.B. Kolton, A. Rosso, E.V. Albano, T. Giamarchi, Short-time relaxation of a driven elastic string in a random medium, Phys. Rev. B 74 (2006) 140201.
[167] A.B. Kolton, G. Schehr, P. Le Doussal, Universal nonstationary dynamics at the depinning transition, Phys. Rev. Lett. 103 (2009) 160602.
[168] P. Chauve, T. Giamarchi, P. Le Doussal, Creep and depinning in disordered media, Phys. Rev. B 62 (2000) 6241.
[169] A. Rosso, A.K. Hartmann, W. Krauth, Depinning of elastic manifolds, Phys. Rev. Lett. 67 (2003) 021602.
[170] J.M. López, J. Schmittbuhl, Anomalous scaling of fracture surfaces, Phys. Rev. E 57 (1998) 6405.
[171] J.J. Ramasco, J.M. López, M.A. Rodriguez, Generic dynamic scaling in kinetic roughening, Phys. Rev. Lett. 84 (2000) 2199.
[172] S. Bustingorry, A.B. Kolton, T. Giamarchi, Thermal rounding of the depinning transition in ultra thin Pt/Co/Pt films, Phys. Rev. B 85 (2012) 214416.
[173] V.V. Randoshkin, Magnetic-field dependence of the domain wall velocity in uniaxial films of iron garnets with various dampings, Sov. Phys., Solid State 37 (1995) 355.
[174] V.Y. Shur, A. Gruverman, N.Y. Ponomarev, E.L. Rumyantsev, N.A. Tonkacheva, Domain structure kinetics in ultrafast polarisation switching in lead germanate, JETP Lett. 53 (1991) 615.
[175] M. Dawber, A. Gruverman, J.F. Scott, Skyrmion model of nano-domain nucleation in ferroelectrics and ferromagnets, J. Phys. Condens. Matter 18 (2006) L71.